

The 5th Egyptian School on High Energy Physics

November 14 – 19, 2015

Zewail City of Science & Technology

Giza, Egypt

Silicon Detectors

Lecture 1

Vito Manzari

National Institute for Nuclear Physics, Bari , Italy

➤ Thanks

to the Organizing Committee and prof. G. Iaselli for the invitation

➤ Outline of these Lectures on Silicon Detectors

Lecture 1

Particle detection and Fundamentals of Semiconductor Detectors

Lecture 2

Semiconductor Detectors, Signal, Noise and Electronics

Lecture 3

CMS and ALICE Silicon Trackers

My slides are based on

Slides I prepared for other lectures

Slides of the lectures given by C. Joram and M. Krammer at the XII ICFA School on Instrumentation

Material found on the web and the authors are then not always recognizable and thus acknowledgeable

Lecture 1

Particle detection and Fundamentals of Semiconductor Detectors

Particle physics, ‘born’ with the discovery of radioactivity and the electron at the end of the 19th century, has become ‘Big Science’ during the last 100 years.

A large variety of instruments and techniques have been (and are) developed for studying the world of particles.

Imaging devices like the cloud chamber, emulsion and the bubble chamber took photographs of the particle tracks.

Logic devices like the Geiger Müller counter, the scintillator or the Cerenkov detector were (and are) widely used.

Through the electronic revolution and the development of new detectors, both traditions merged into the ‘electronics image’ in the 1970ies.

Particle detectors with up to millions of readout channels are currently operated.

Various aspects of the penetration of charged particles in matter have occupied the thoughts of some of the finest physicists of the last century.

E.g. Thomson 1903, Rutherford 1911, Bohr 1913, 1915, 1948, Bethe 1930, 1932, Mott, 1931, Bloch 1933, Fermi 1940, Landau 1944

In the first half of the 20th century, the energy loss of the charged particles and the related stopping power of materials was the prime issue.

Nowadays, the actual amount of scintillation light and/or charge produced by the passing particle, and the fluctuations of these quantities, are the important quantity because these are the quantities producing the signals in particle detectors and their fluctuations are responsible for the resolution limits of the detectors.

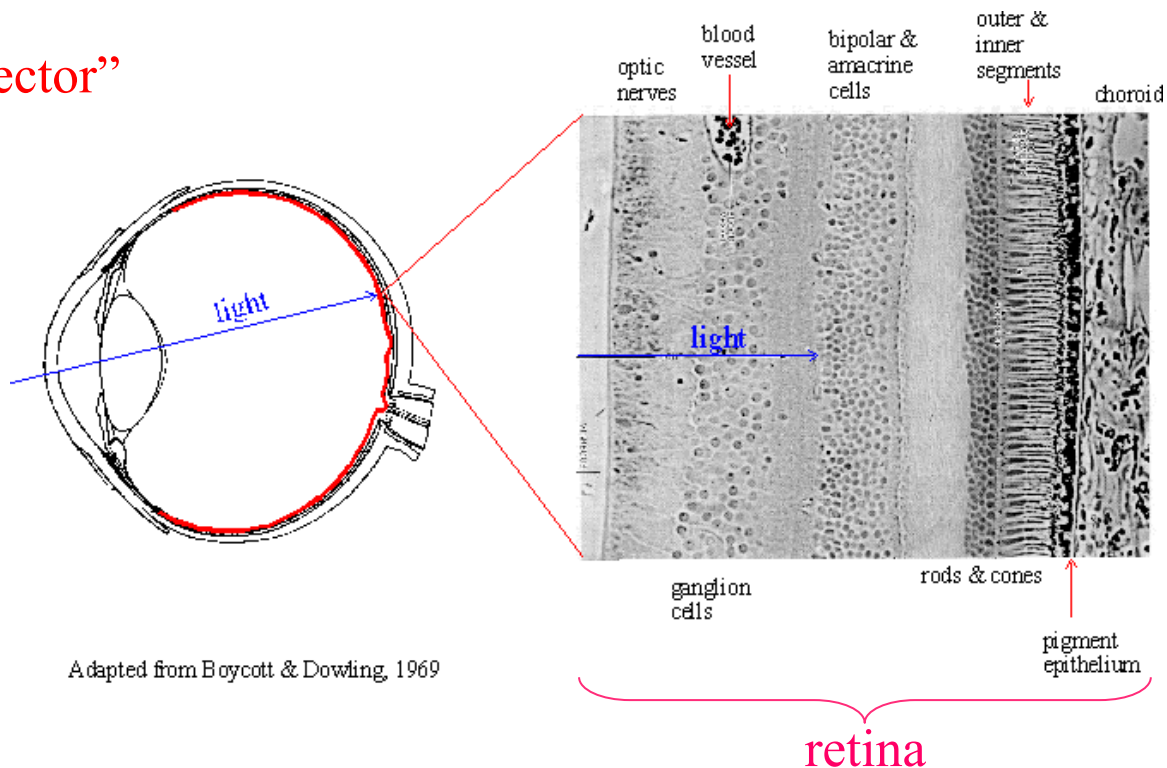
In the following, we will briefly review the basic mechanisms that are responsible for the creation of excitation and ionization.

“The oldest particle (photon) detector”
built many billion times

- Good spatial resolution
- Very large dynamic range (1:10⁶)
Automatic threshold adaptation
- Energy (wavelength) discrimination
- Modest sensitivity

500 to 900 photons must arrive at the eye every second for our brain to register a conscious signal

- Modest speed
Data taking rate $\sim 10\text{Hz}$ (incl. processing)



Some important definitions and units

$$E^2 = \vec{p}^2 c^2 + m_0^2 c^4$$

- energy E : measure in eV
- momentum p : measure in eV/c
- mass m_0 : measure in eV/c²

$$\beta = \frac{v}{c} \quad (0 \leq \beta < 1) \quad \gamma = \frac{1}{\sqrt{1 - \beta^2}} \quad (1 \leq \gamma < \infty)$$

$$E = m_0 \gamma c^2 \quad p = m_0 \gamma \beta c \quad \beta = \frac{pc}{E}$$

1 eV is a tiny portion of energy: 1 eV = 1.6 · 10⁻¹⁹ J



$$m_{bee} = 1\text{g} = 5.8 \cdot 10^{32} \text{ eV}/c^2$$

$$v_{bee} = 1\text{m/s} \rightarrow E_{bee} = 10^{-3} \text{ J} = 6.25 \cdot 10^{15} \text{ eV}$$

$$E_{LHC} = 14 \cdot 10^{12} \text{ eV (two colliding proton)}$$

To be fair with LHC...

Total stored beam energy: $E_{total} = 10^{14} \text{ protons} \cdot 7 \cdot 10^{12} \text{ eV} \approx 7 \cdot 10^{26} \text{ eV} \approx 1 \cdot 10^8 \text{ J}$

this corresponds to a



$$m_{truck} = 100 \text{ T}$$

$$v_{truck} = 120 \text{ km/h}$$

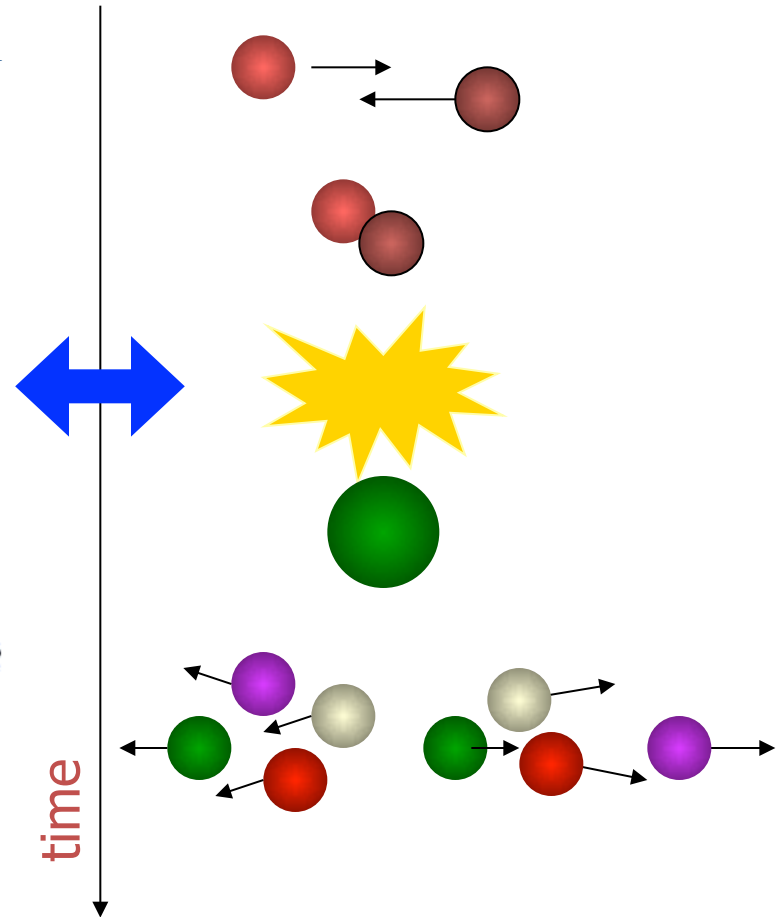
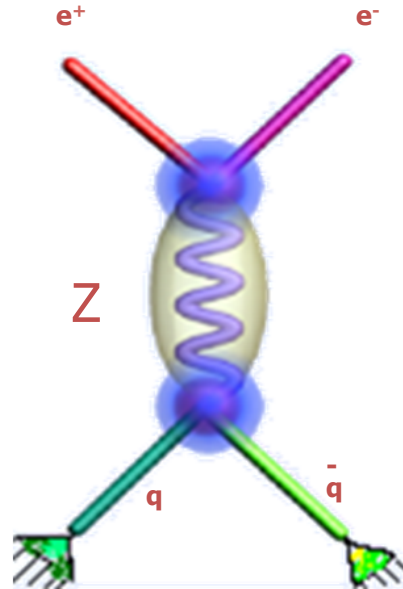
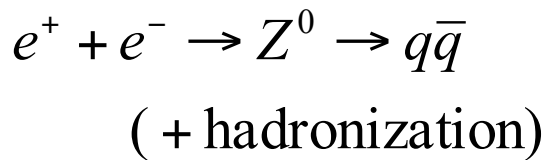
Stored energy in LHC magnets ~ 1 GJ



$$m_{747} = 400 \text{ T}$$

$$v_{747} = 255 \text{ km/h}$$

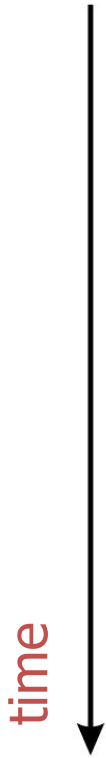
- Idealistic views of an elementary particle reaction



Usually we can not ‘see’ the reaction itself, but only the end products of the reaction

In order to reconstruct the reaction mechanism and the properties of the involved particles, we want the maximum information about the **end products!**

Higgs production...in the macroscopic world



- The 'ideal' particle detector should provide

coverage of full solid angle

no cracks, fine segmentation

measurement of momentum and/or energy

detect, track and identify all particles

mass, charge

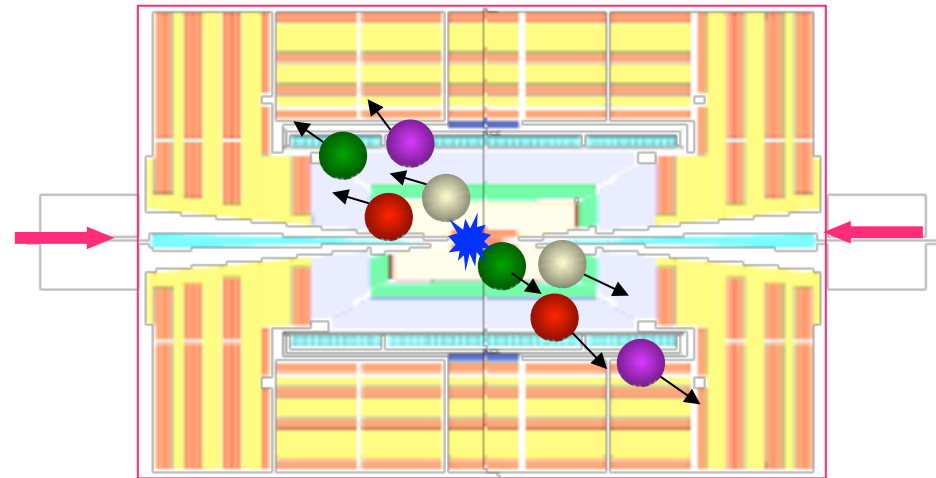
fast response

no dead time

practical limitations

technology, space, budget

e^+e^- , ep , pp , $p\bar{p}$, pA , AA



end products

- charged particles
- neutral particles
- photons

- Particles are detected via their interaction with matter
- Many different physical principles are involved, mainly of electromagnetic nature

Finally we will always observe ionization and/or excitation of matter

Baryon Summary Table

This short table gives the name, the quantum numbers (where known), and the status of baryons in the Review. Only the baryons with 3 or 4 star status are included in the Baryon Summary Table. Due to insufficient data or uncertain interpretation, the other entries in the table are not established baryons. The names with masses are of baryons that decay strongly. The spin parity J^P (when known) is given with each particle. For the strongly decaying particles, the J^P values are considered to be part of the names.

Particle	Quantum Numbers	Name	Quantum Numbers	Name	Quantum Numbers	Name	Quantum Numbers	Name	Quantum Numbers	Name	
p	$1/2^+$	****	$\Delta(1232)$	$3/2^+$	****	Σ^+	$1/2^+$	****	Ξ^0	$1/2^+$	****
n	$1/2^+$	****	$\Delta(1600)$	$3/2^+$	****	Σ^0	$1/2^+$	****	Ξ^-	$1/2^+$	****
$N(1440)$	$1/2^+$	****	$\Delta(1620)$	$1/2^-$	****	Σ^-	$1/2^+$	****	$\Xi(1530)$	$3/2^+$	****
$N(1520)$	$3/2^-$	****	$\Delta(1700)$	$3/2^-$	****	$\Sigma(1385)$	$3/2^+$	****	$\Xi(1620)$	*	
$N(1535)$	$1/2^-$	****	$\Delta(1750)$	$1/2^+$	*	$\Sigma(1480)$	*		$\Xi(1690)$	*	
$N(1650)$	$1/2^-$	****	$\Delta(1900)$	$1/2^-$	**	$\Sigma(1560)$	**		$\Xi(1820)$	$3/2^-$	****
$N(1675)$	$5/2^-$	****	$\Delta(1905)$	$5/2^+$	****	$\Sigma(1580)$	$3/2^-$	*	$\Xi(1950)$	****	
$N(1680)$	$5/2^+$	****	$\Delta(1910)$	$1/2^+$	*	$\Sigma(1620)$	$1/2^-$	*	$\Xi(2030)$	$\geq \frac{5}{2}^?$	*
$N(1685)$	*		$\Delta(1920)$	$3/2^+$	****	$\Sigma(1660)$	$1/2^+$	**	$\Xi(2120)$	*	
$N(1700)$	$3/2^-$	****	$\Delta(1930)$	$5/2^-$	****	$\Sigma(1670)$	$3/2^-$	****	$\Xi(2250)$	**	
$N(1710)$	$1/2^+$	****	$\Delta(1940)$	$3/2^-$	**	$\Sigma(1690)$	**		$\Xi(2370)$	**	
$N(1720)$	$3/2^+$	****	$\Delta(1950)$	$7/2^+$	****	$\Sigma(1750)$	$1/2^-$	****	$\Xi(2500)$	**	
$N(1860)$	$5/2^+$	****	$\Delta(2000)$	$1/2^-$	****	$\Sigma(1880)$	$1/2^+$	**	$\Xi(2790)$	$1/2^-$	****
$N(1875)$	$3/2^-$	****	$\Delta(2040)$	$9/2^-$	****	$\Sigma(1940)$	$3/2^-$	**	$\Xi(2815)$	$3/2^-$	****
$N(1880)$	$1/2^+$	****	$\Delta(2100)$	$7/2^+$	****	$\Sigma(2030)$	$7/2^+$	****	$\Xi(2980)$	**	
$N(1895)$	$1/2^-$	**	$\Delta(2300)$	$7/2^-$	**	$\Sigma(2100)$	$7/2^-$	*	$\Xi(3055)$	**	
$N(1900)$	$3/2^+$	****	$\Delta(2300)$	$9/2^+$	**	$\Sigma(2150)$	$9/2^+$	**	$\Xi(3080)$	**	
$N(1990)$	$7/2^+$	****	$\Delta(2400)$	$9/2^-$	**	$\Sigma(2000)$	$1/2^-$	**	$\Xi(3123)$	*	
$N(2000)$	$5/2^+$	**	$\Delta(2420)$	$11/2^+$	****	$\Sigma(2030)$	$7/2^+$	****	$\Xi(3270)$	$1/2^+$	****
$N(2040)$	$3/2^+$	**	$\Delta(2420)$	$11/2^+$	****	$\Sigma(2030)$	$7/2^+$	****	$\Xi(3370)$	$3/2^+$	****
$N(2060)$	$5/2^-$	**	$\Delta(2420)$	$11/2^+$	****	$\Sigma(2100)$	$7/2^-$	*	$\Xi(3400)$	*	
$N(2100)$	$1/2^+$	**	$\Delta(2420)$	$11/2^+$	****	$\Sigma(2100)$	$7/2^-$	*	$\Xi(3470)$	$3/2^+$	****
$N(2120)$	$3/2^-$	**	$\Delta(2420)$	$11/2^+$	****	$\Sigma(2100)$	$7/2^-$	*	$\Xi(3500)$	*	
$N(2190)$	$7/2^-$	****	$\Delta(2420)$	$11/2^+$	****	$\Sigma(2100)$	$7/2^-$	*	$\Xi(3500)$	*	
$N(2220)$	$9/2^+$	****	$\Delta(2420)$	$11/2^+$	****	$\Sigma(2100)$	$7/2^-$	*	$\Xi(3500)$	*	
$N(2250)$	$9/2^-$	****	$\Delta(2420)$	$11/2^+$	****	$\Sigma(2100)$	$7/2^-$	*	$\Xi(3500)$	*	
$N(2300)$	$1/2^+$	**	$\Delta(2420)$	$11/2^+$	****	$\Sigma(2100)$	$7/2^-$	*	$\Xi(3500)$	*	
$N(2570)$	$5/2^-$	**	$\Delta(2420)$	$11/2^+$	****	$\Sigma(2100)$	$7/2^-$	*	$\Xi(3500)$	*	
$N(2600)$	$11/2^-$	****	$\Delta(2420)$	$11/2^+$	****	$\Sigma(2100)$	$7/2^-$	*	$\Xi(3500)$	*	
$N(2700)$	$13/2^+$	**	$\Delta(2420)$	$11/2^+$	****	$\Sigma(2100)$	$7/2^-$	*	$\Xi(3500)$	*	

There are hundreds of particles ... however most of them are so short-lived that we'll never see them directly in our detectors.

Track length: $l_{\text{track}} = v\tau = c\beta\gamma\tau_0$ with τ_0 being the lifetime at rest. Only if l_{track} (at GeV scale) ≥ 1 mm, we have a chance to measure them

Meson Summary Table

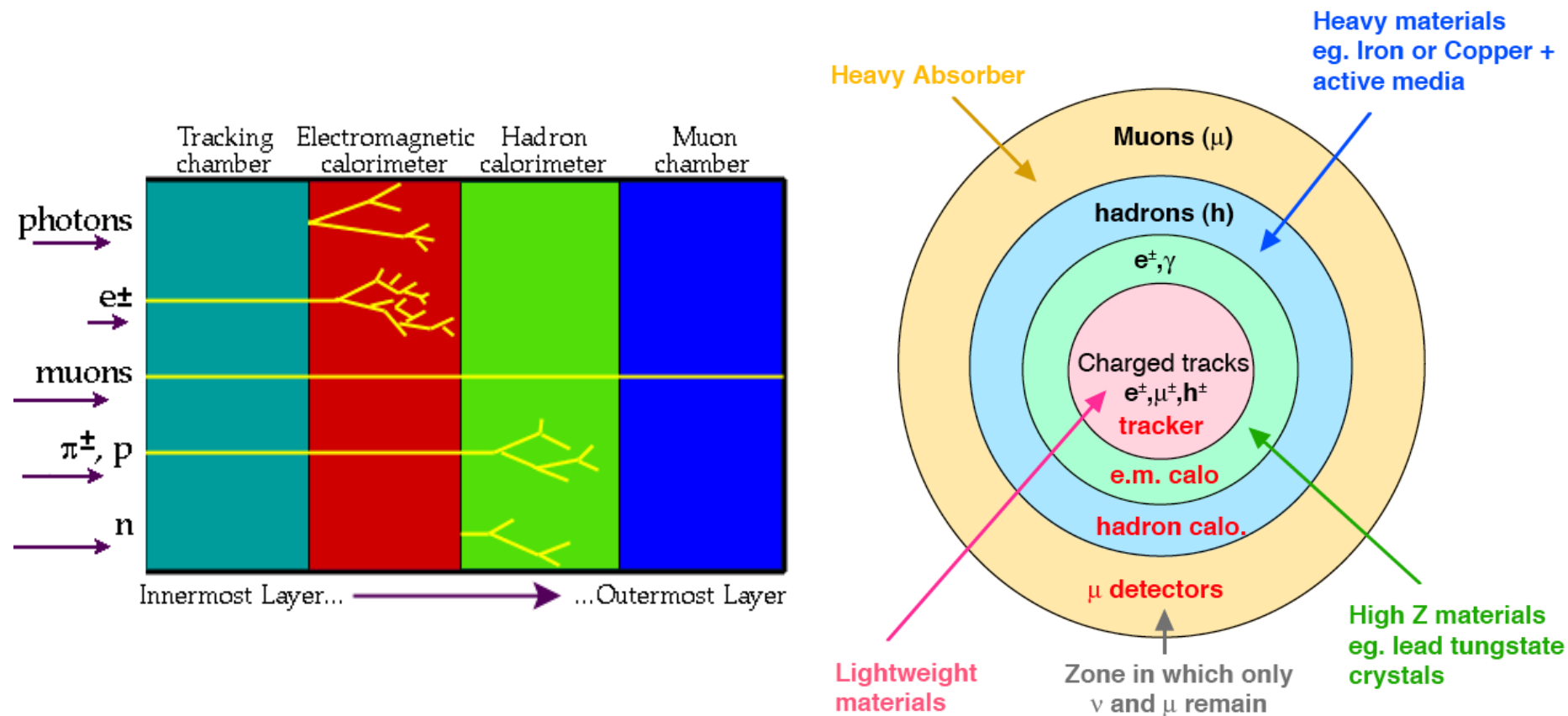
See also the table of suggested $q\bar{q}$ quark model assignments in the Quark Model section.
 • Indicates particles that appear in the preceding Meson Summary Table. We do not regard the other entries as being established.

LIGHT UNFLAVORED ($S=C=B=0$)		STRANGE ($S=\pm 1, C=B=0$)		CHARMED, STRANGE ($C=S=\pm 1$)		$c\bar{c}$ $\bar{c}c$	
$\bar{\rho}(J^PC)$	$\rho(J^PC)$	$\bar{K}(J^PC)$	$K(J^PC)$	$\bar{K}^*(J^PC)$	$K^*(J^PC)$	$\bar{c}c$	$\bar{c}c$
π^{\pm}	$1^-(0^-)$	$\pi_2(1670)$	$1^-(2^-)$	K^{\pm}	$1/2(0^-)$	D_1^*	$0^-(0^-)$
π^0	$1^-(0^-)$	$\rho(1680)$	$0^-(1^-)$	K^0	$1/2(0^-)$	D_s^{*+}	$0^-(0^-)$
η	$0^-(0^-)$	$\rho(1690)$	$1^+(3^-)$	K_S^0	$1/2(0^-)$	D_s^{*0}	$0^-(0^-)$
$\eta(500)$	$0^-(0^+)$	$\rho(1700)$	$1^+(1^-)$	K_L^0	$1/2(0^-)$	$D_{s1}^*(2317)^{\pm}$	$0^-(2^+)$
$\eta(770)$	$1^+(1^-)$	$\rho(1700)$	$1^-(2^+)$	$K_1^*(800)$	$1/2(1^+)$	$D_{s1}(2460)^{\pm}$	$0^-(1^+)$
$\omega(782)$	$0^-(1^-)$	$\rho(1710)$	$0^+(0^+)$	$K_2^*(892)$	$1/2(2^+)$	$D_{s1}(2536)^{\pm}$	$0^-(1^+)$
$\eta(958)$	$0^-(0^+)$	$\rho(1760)$	$0^+(0^+)$	$K_2^*(1270)$	$1/2(2^+)$	$D_{s2}(2573)$	$0^-(2^+)$
$\phi(980)$	$0^-(0^+)$	$\rho(1800)$	$1^-(0^+)$	$K_1^*(1400)$	$1/2(1^+)$	$D_{s1}^*(2700)^{\pm}$	$0^-(1^+)$
$\omega(980)$	$1^-(0^+)$	$\phi(1810)$	$0^+(2^+)$	$K_1^*(1410)$	$1/2(1^+)$	$D_{s1}^*(2860)^{\pm}$	$0^-(2^+)$
$\omega(1020)$	$0^-(1^-)$	$\chi(1835)$	$?^?(2^-)$	$K_1^*(1430)$	$1/2(1^+)$	$D_{s1}(3040)^{\pm}$	$0^-(2^+)$
$\eta(1170)$	$0^-(1^+)$	$\phi(1850)$	$0^-(3^-)$	$K_1^*(1430)$	$1/2(2^+)$	BOTTOM ($B=\pm 1$)	
$\eta(1295)$	$1^-(1^+)$	$\eta(1875)$	$0^-(2^-)$	$K(1460)$	$1/2(0^-)$	B^+	$1/2(0^-)$
$\eta(1295)$	$1^-(1^+)$	$\eta(1875)$	$1^-(2^-)$	$K(1580)$	$1/2(2^-)$	B^0	$1/2(0^-)$
$\eta(1295)$	$0^-(1^+)$	$\eta(1910)$	$1^-(1^-)$	$K(1630)$	$1/2(2^+)$	B^+	B^0 ADMIXTURE
$\eta(1295)$	$0^-(0^+)$	$\eta(1910)$	$0^-(2^+)$	$K_1(1650)$	$1/2(1^+)$	B^+	B^0 ADMIXTURE
$\eta(1295)$	$0^-(0^+)$	$\eta(1990)$	$1^-(3^-)$	$K_1^*(1680)$	$1/2(1^+)$	B^+	B^0 ADMIXTURE
$\eta(1300)$	$1^-(0^+)$	$\eta(1990)$	$1^-(3^-)$	$K_1^*(1770)$	$1/2(2^+)$	V_{cb} and V_{cb} CKM Ma	$X(4160)$
$\eta(1300)$	$1^-(0^+)$	$\eta(2030)$	$0^-(2^+)$	$K_1^*(1770)$	$1/2(2^+)$	V_{cb} and V_{cb} CKM Ma	$X(4260)$
$\eta(1300)$	$1^-(0^+)$	$\eta(2030)$	$0^-(2^+)$	$K_1^*(1770)$	$1/2(2^+)$	V_{cb} and V_{cb} CKM Ma	$X(4360)$
$\eta(1300)$	$1^-(0^+)$	$\eta(2030)$	$0^-(2^+)$	$K_1^*(1770)$	$1/2(2^+)$	V_{cb} and V_{cb} CKM Ma	$X(4560)$
$\eta(1300)$	$1^-(0^+)$	$\eta(2030)$	$0^-(2^+)$	$K_1^*(1770)$	$1/2(2^+)$	V_{cb} and V_{cb} CKM Ma	$X(4660)$
$\eta(1300)$	$1^-(0^+)$	$\eta(2030)$	$0^-(2^+)$	$K_1^*(1770)$	$1/2(2^+)$	V_{cb} and V_{cb} CKM Ma	$X(4760)$
$\eta(1300)$	$1^-(0^+)$	$\eta(2030)$	$0^-(2^+)$	$K_1^*(1770)$	$1/2(2^+)$	V_{cb} and V_{cb} CKM Ma	$X(4860)$
$\eta(1300)$	$1^-(0^+)$	$\eta(2030)$	$0^-(2^+)$	$K_1^*(1770)$	$1/2(2^+)$	V_{cb} and V_{cb} CKM Ma	$X(4960)$
$\eta(1300)$	$1^-(0^+)$	$\eta(2030)$	$0^-(2^+)$	$K_1^*(1770)$	$1/2(2^+)$	V_{cb} and V_{cb} CKM Ma	$X(5060)$
$\eta(1300)$	$1^-(0^+)$	$\eta(2030)$	$0^-(2^+)$	$K_1^*(1770)$	$1/2(2^+)$	V_{cb} and V_{cb} CKM Ma	$X(5160)$
$\eta(1300)$	$1^-(0^+)$	$\eta(2030)$	$0^-(2^+)$	$K_1^*(1770)$	$1/2(2^+)$	V_{cb} and V_{cb} CKM Ma	$X(5260)$
$\eta(1300)$	$1^-(0^+)$	$\eta(2030)$	$0^-(2^+)$	$K_1^*(1770)$	$1/2(2^+)$	V_{cb} and V_{cb} CKM Ma	$X(5360)$
$\eta(1300)$	$1^-(0^+)$	$\eta(2030)$	$0^-(2^+)$	$K_1^*(1770)$	$1/2(2^+)$	V_{cb} and V_{cb} CKM Ma	$X(5460)$
$\eta(1300)$	$1^-(0^+)$	$\eta(2030)$	$0^-(2^+)$	$K_1^*(1770)$	$1/2(2^+)$	V_{cb} and V_{cb} CKM Ma	$X(5560)$
$\eta(1300)$	$1^-(0^+)$	$\eta(2030)$	$0^-(2^+)$	$K_1^*(1770)$	$1/2(2^+)$	V_{cb} and V_{cb} CKM Ma	$X(5660)$
$\eta(1300)$	$1^-(0^+)$	$\eta(2030)$	$0^-(2^+)$	$K_1^*(1770)$	$1/2(2^+)$	V_{cb} and V_{cb} CKM Ma	$X(5760)$
$\eta(1300)$	$1^-(0^+)$	$\eta(2030)$	$0^-(2^+)$	$K_1^*(1770)$	$1/2(2^+)$	V_{cb} and V_{cb} CKM Ma	$X(5860)$
$\eta(1300)$	$1^-(0^+)$	$\eta(2030)$	$0^-(2^+)$	$K_1^*(1770)$	$1/2(2^+)$	V_{cb} and V_{cb} CKM Ma	$X(5960)$
$\eta(1300)$	$1^-(0^+)$	$\eta(2030)$	$0^-(2^+)$	$K_1^*(1770)$	$1/2(2^+)$	V_{cb} and V_{cb} CKM Ma	$X(6060)$
$\eta(1300)$	$1^-(0^+)$	$\eta(2030)$	$0^-(2^+)$	$K_1^*(1770)$	$1/2(2^+)$	V_{cb} and V_{cb} CKM Ma	$X(6160)$
$\eta(1300)$	$1^-(0^+)$	$\eta(2030)$	$0^-(2^+)$	$K_1^*(1770)$	$1/2(2^+)$	V_{cb} and V_{cb} CKM Ma	$X(6260)$
$\eta(1300)$	$1^-(0^+)$	$\eta(2030)$	$0^-(2^+)$	$K_1^*(1770)$	$1/2(2^+)$	V_{cb} and V_{cb} CKM Ma	$X(6360)$
$\eta(1300)$	$1^-(0^+)$	$\eta(2030)$	$0^-(2^+)$	$K_1^*(1770)$	$1/2(2^+)$	V_{cb} and V_{cb} CKM Ma	$X(6460)$
$\eta(1300)$	$1^-(0^+)$	$\eta(2030)$	$0^-(2^+)$	$K_1^*(1770)$	$1/2(2^+)$	V_{cb} and V_{cb} CKM Ma	$X(6560)$
$\eta(1300)$	$1^-(0^+)$	$\eta(2030)$	$0^-(2^+)$	$K_1^*(1770)$	$1/2(2^+)$	V_{cb} and V_{cb} CKM Ma	$X(6660)$
$\eta(1300)$	$1^-(0^+)$	$\eta(2030)$	$0^-(2^+)$	$K_1^*(1770)$	$1/2(2^+)$	V_{cb} and V_{cb} CKM Ma	$X(6760)$
$\eta(1300)$	$1^-(0^+)$	$\eta(2030)$	$0^-(2^+)$	$K_1^*(1770)$	$1/2(2^+)$	V_{cb} and V_{cb} CKM Ma	$X(6860)$
$\eta(1300)$	$1^-(0^+)$	$\eta(2030)$	$0^-(2^+)$	$K_1^*(1770)$	$1/2(2^+)$	V_{cb} and V_{cb} CKM Ma	$X(6960)$
$\eta(1300)$	$1^-(0^+)$	$\eta(2030)$	$0^-(2^+)$	$K_1^*(1770)$	$1/2(2^+)$	V_{cb} and V_{cb} CKM Ma	$X(7060)$
$\eta(1300)$	$1^-(0^+)$	$\eta(2030)$	$0^-(2^+)$	$K_1^*(1770)$	$1/2(2^+)$	V_{cb} and V_{cb} CKM Ma	$X(7160)$
$\eta(1300)$	$1^-(0^+)$	$\eta(2030)$	$0^-(2^+)$	$K_1^*(1770)$	$1/2(2^+)$	V_{cb} and V_{cb} CKM Ma	$X(7260)$
$\eta(1300)$	$1^-(0^+)$	$\eta(2030)$	$0^-(2^+)$	$K_1^*(1770)$	$1/2(2^+)$	V_{cb} and V_{cb} CKM Ma	$X(7360)$
$\eta(1300)$	$1^-(0^+)$	$\eta(2030)$	$0^-(2^+)$	$K_1^*(1770)$	$1/2(2^+)$	V_{cb} and V_{cb} CKM Ma	$X(7460)$
$\eta(1300)$	$1^-(0^+)$	$\eta(2030)$	$0^-(2^+)$	$K_1^*(1770$			

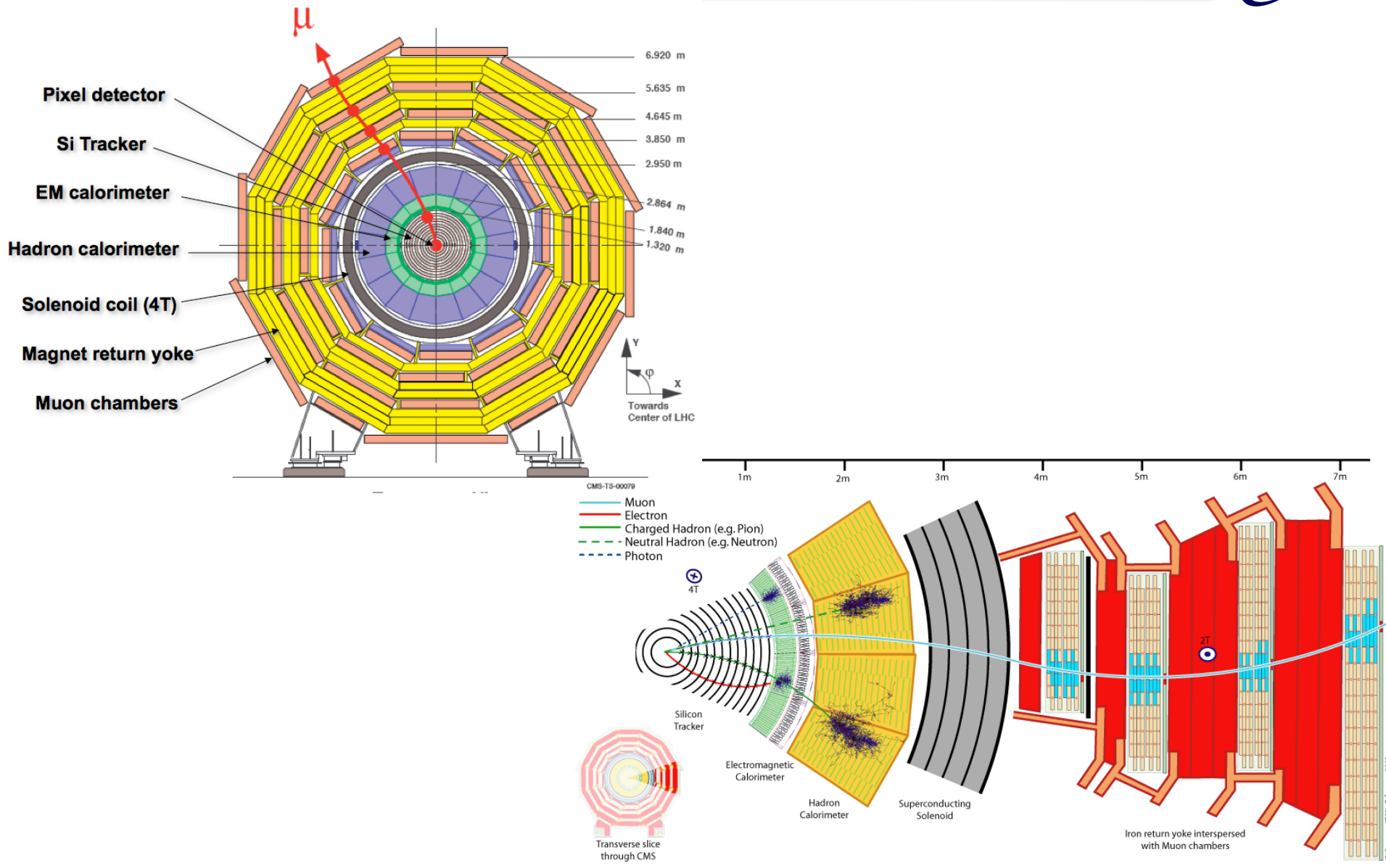
Basic Concept of HEP Detectors

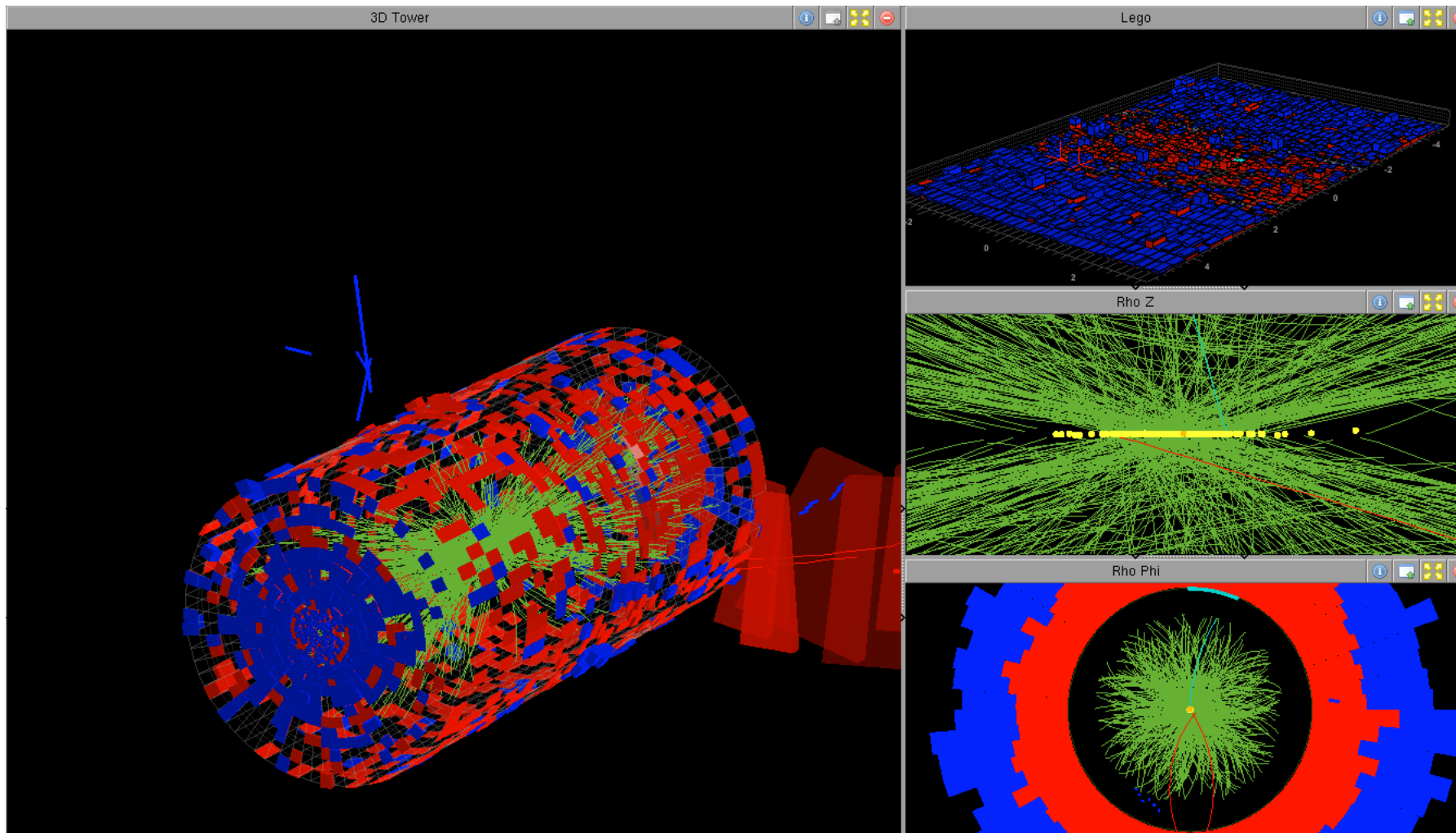
- Detectors are designed to be able to distinguish between the different types of object ($e^\pm, \gamma, \mu^\pm, \text{hadrons}$)

⇒ Many HEP detectors have an onion like structure:



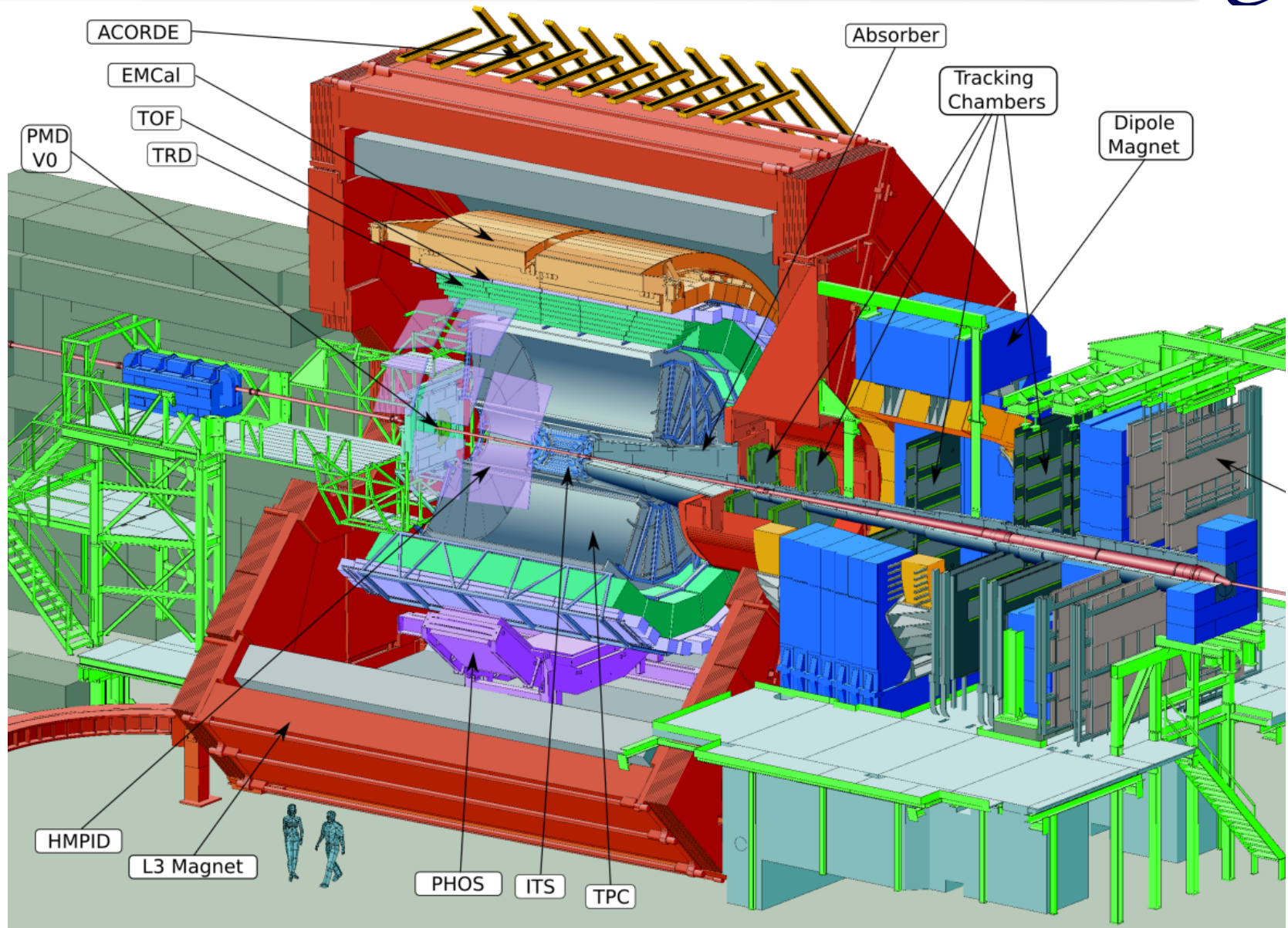
The CMS Detector

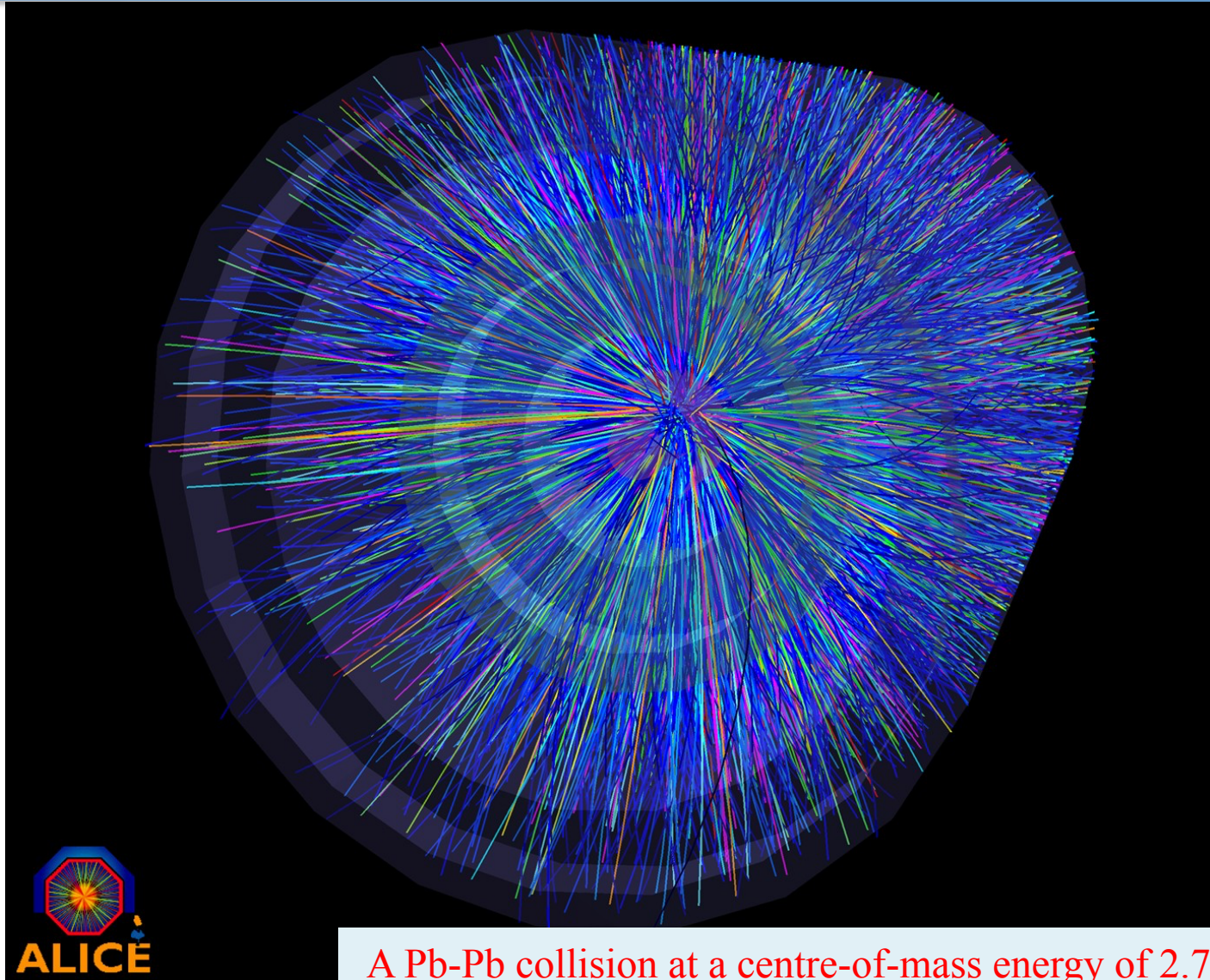




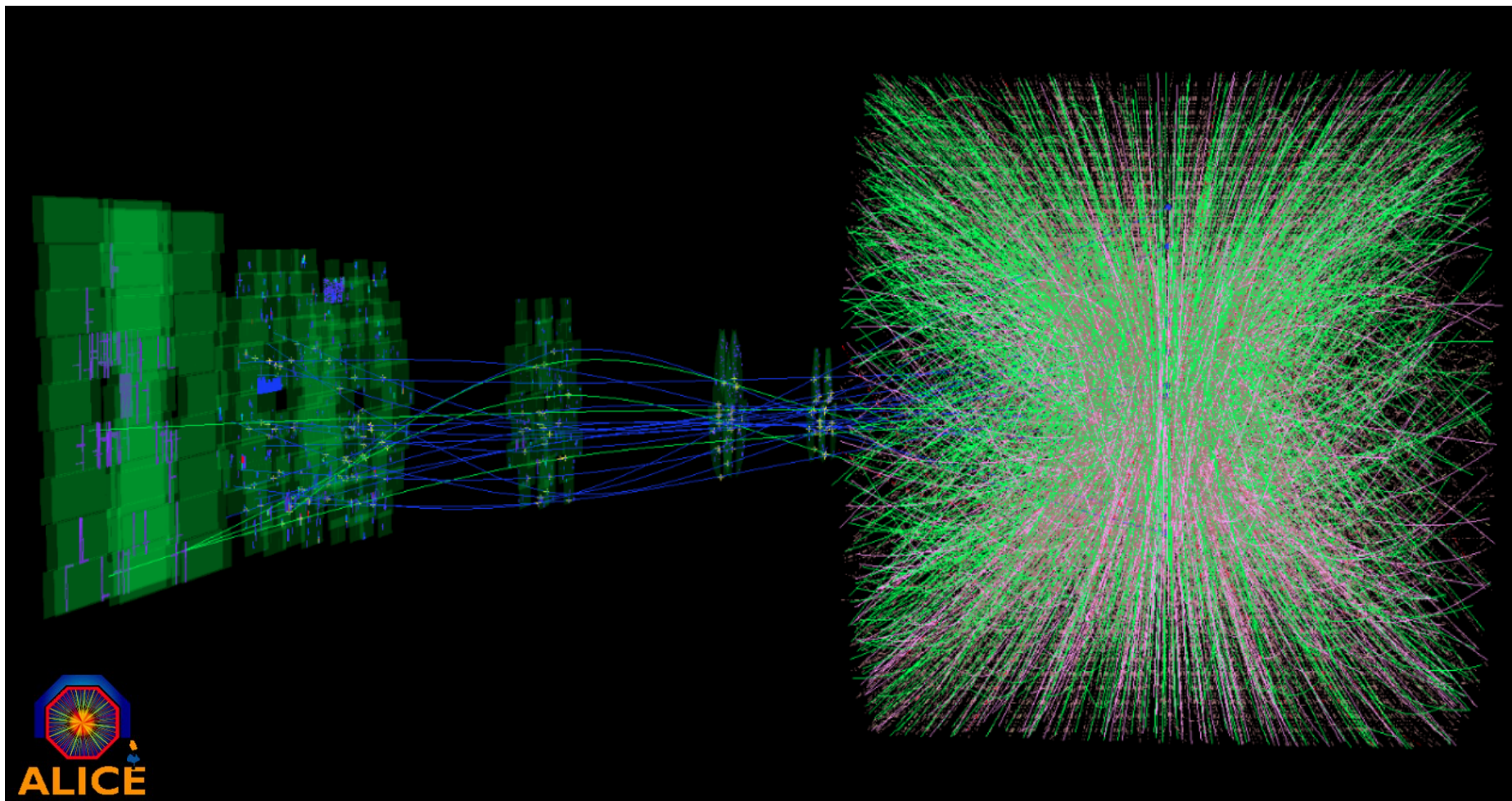
The exceptional performance of the Tracker can be seen in this event display that shows **78 reconstructed vertices** in one beam crossing, obtained from a special high-pileup run

The ALICE Detector





A Pb-Pb collision at a centre-of-mass energy of 2.76 TeV per nucleon pair: thousand of tracks are produced and recorded



A Pb-Pb collision at a centre-of-mass energy of 2.76 TeV per nucleon pair with muon tracks in the forward muon spectrometer

Every effect of particles or radiation can be used as a working principle for a particle detector.

Precise knowledge of the processes leading to signals in particle detectors is necessary.

The detectors are nowadays working close to the limits of theoretically achievable measurement accuracy – even in large systems

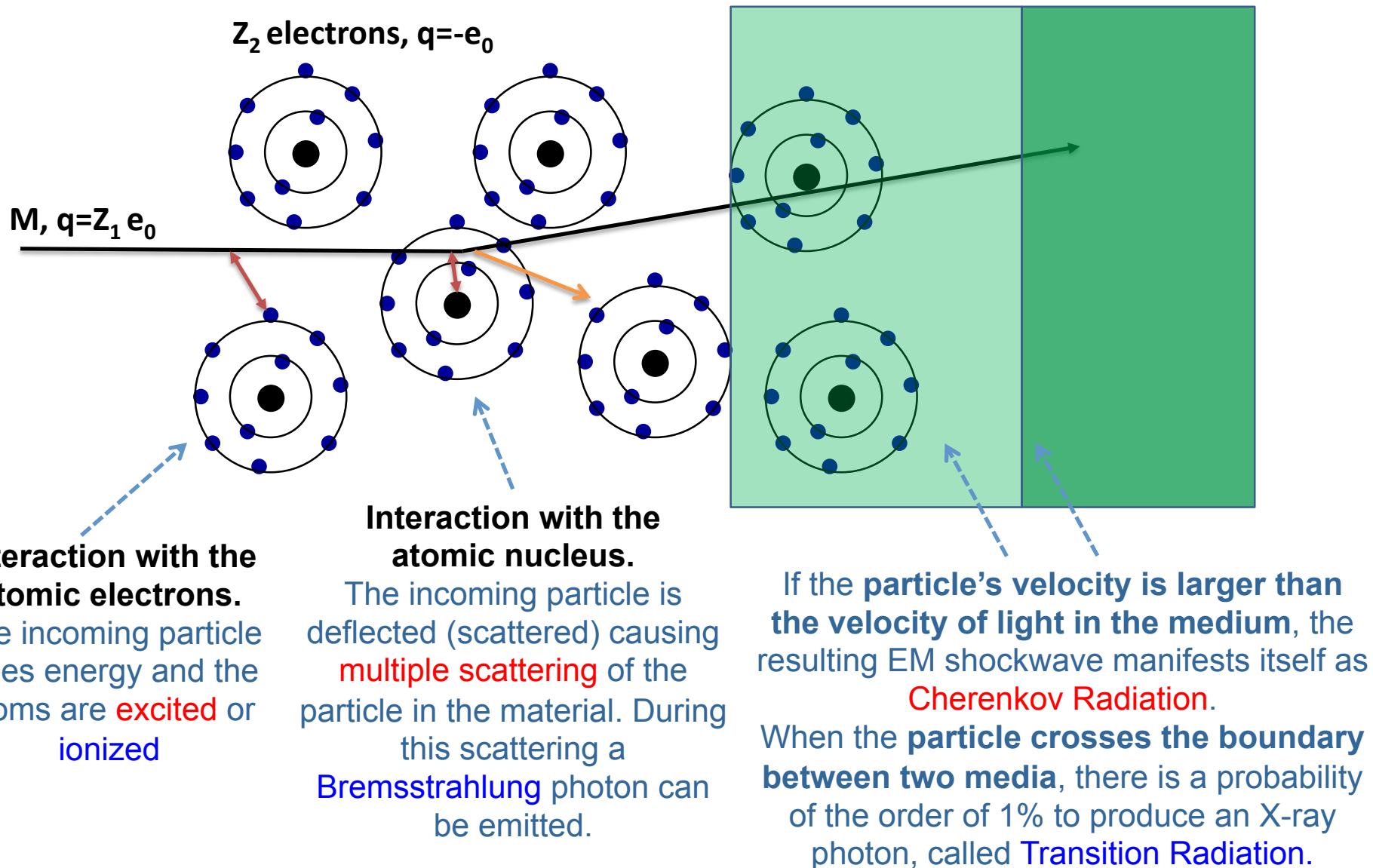
Different type of interactions for charged and neutral particles

Difference “scale” of processes for electromagnetic and strong Interactions

- Detection of γ -rays (Photo/Compton effect, pair production)
- Detection of neutrons (strong interaction)
- **Detection of charged particles**
 - **Ionization**, Bremsstrahlung, Cherenkov, Transition Radiation

- Ultimately all detectors end up detecting charged particles:
 - Photons are detected via electrons produced through:
 - Photoelectric effect
 - Compton effect
 - **e^+e^- pair production** (dominates for $E > 5\text{GeV}$)
 - Neutrons are detected through transfer of energy to charged particles in the detector medium (shower of secondary hadrons)
- Charged particles are detected via electromagnetic interaction with electrons or nuclei in the detector material:
 - Elastic scattering from nuclei \rightarrow change of direction
 - Inelastic collisions with atomic electrons \rightarrow energy loss

EM Interaction of charged particles with Matter



- **Elastic Scattering**

An incoming particle with charge z interacts elastically with a target of nuclear charge Z .

The cross-section for this e.m. process is

$$\frac{d\sigma}{d\Omega}(\theta) = 4zZr_e^2 \left(\frac{m_e c}{\beta p} \right)^2 \frac{1}{\sin^4 \theta/2} \quad \text{Rutherford formula}$$

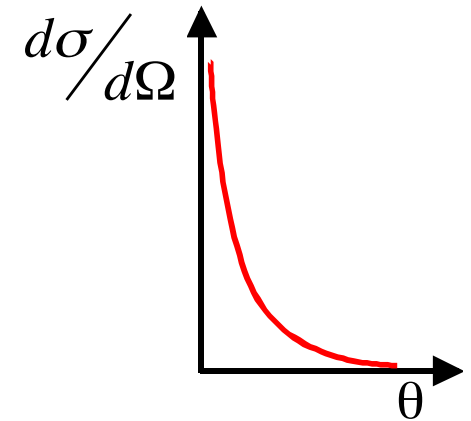
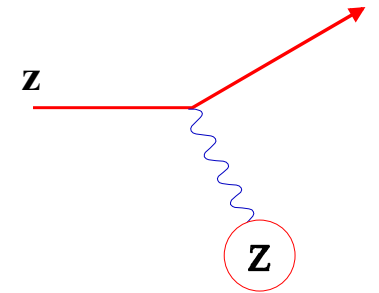
- **Approximation**

Non-relativistic

No spins

- Average scattering angle $\langle \theta \rangle = 0$

- Cross-section for $\theta \rightarrow 0$ infinite!



Scattering does not lead to significant energy loss because nuclei are heavy

In a sufficiently thick material layer a particle will undergo

Multiple (Elastic) Scattering

The final displacement and direction are the result of many independent random scatterings

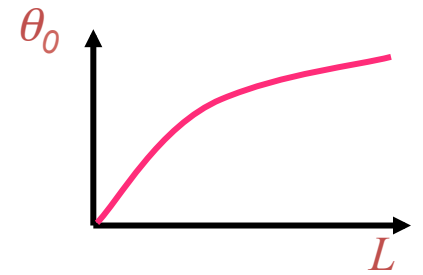
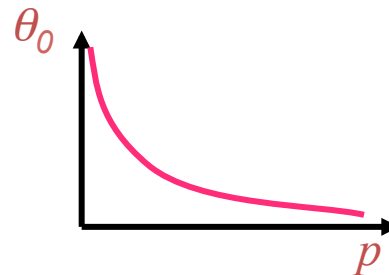
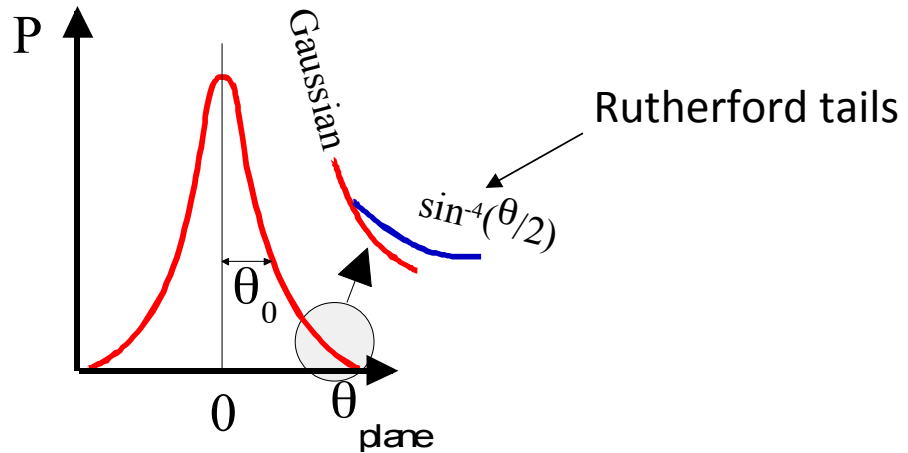
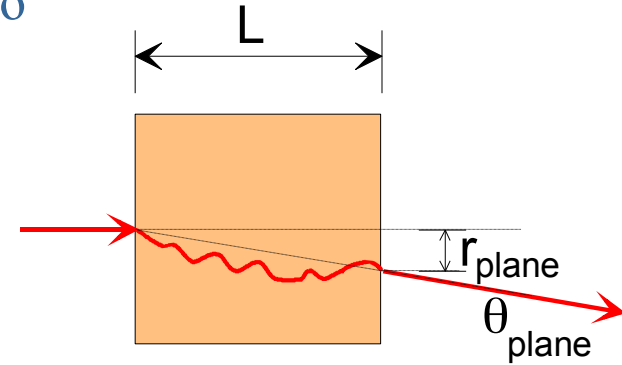
Central limit theorem

Gaussian distribution

$$\theta_0 = \theta_{plane}^{RMS} = \sqrt{\langle \theta_{plane}^2 \rangle} = \frac{1}{\sqrt{2}} \theta_{space}^{RMS}$$

Approximation $\theta_0 \propto \frac{1}{p} \sqrt{\frac{L}{X_0}}$

p = momentum of the particle
 L = thickness of the traversed material
 X_0 = radiation length of the medium

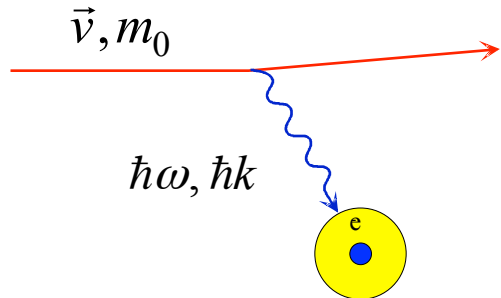


Detection of charged particles

- Particles can only be detected if they deposit energy in matter

How do they lose energy in matter?

Discrete collisions with the atomic electrons of the absorber material



The diagram shows a red arrow representing an incident particle with velocity \vec{v} and mass m_0 . A blue wavy arrow labeled $\hbar\omega, \hbar k$ points from the particle to a yellow circle representing an electron with a blue dot in the center and labeled 'e'.

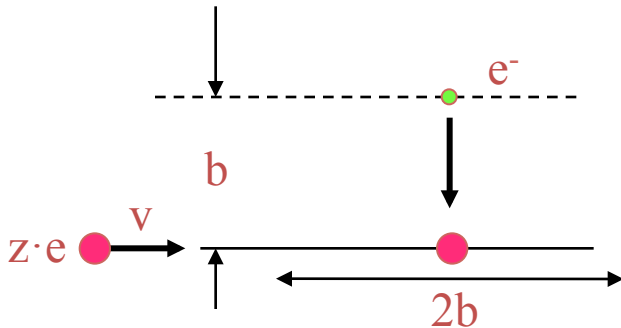
$$\left\langle \frac{dE}{dx} \right\rangle = - \int_0^\infty N E \frac{d\sigma}{dE} \hbar d\omega \quad \left(\omega = 2\pi f = 2\pi \cdot \frac{c}{\lambda} \right)$$

N = electron density

If $\hbar\omega, \hbar k$ are in the right range \Rightarrow ionization

Collisions with nuclei are not important ($m_e \ll m_N$) for energy loss

- Average differential energy loss $\left\langle \frac{dE}{dx} \right\rangle$... making Bethe-Bloch plausible
- Energy loss at a single encounter with an electron



$$F_c = \frac{ze^2}{b^2} \quad \Delta t = \frac{2b}{v} \quad \Delta p_e = F_c \Delta t$$

$$\Delta E_e = \frac{(\Delta p_e)^2}{2m_e} = \frac{2z^2 e^4}{b^2 v^2 m_e} = \frac{2r_e^2 m_e c^2 z^2}{b^2} \cdot \frac{1}{\beta^2}$$

Introduced classical electron radius $r_e = \frac{e^2}{m_e c^2}$

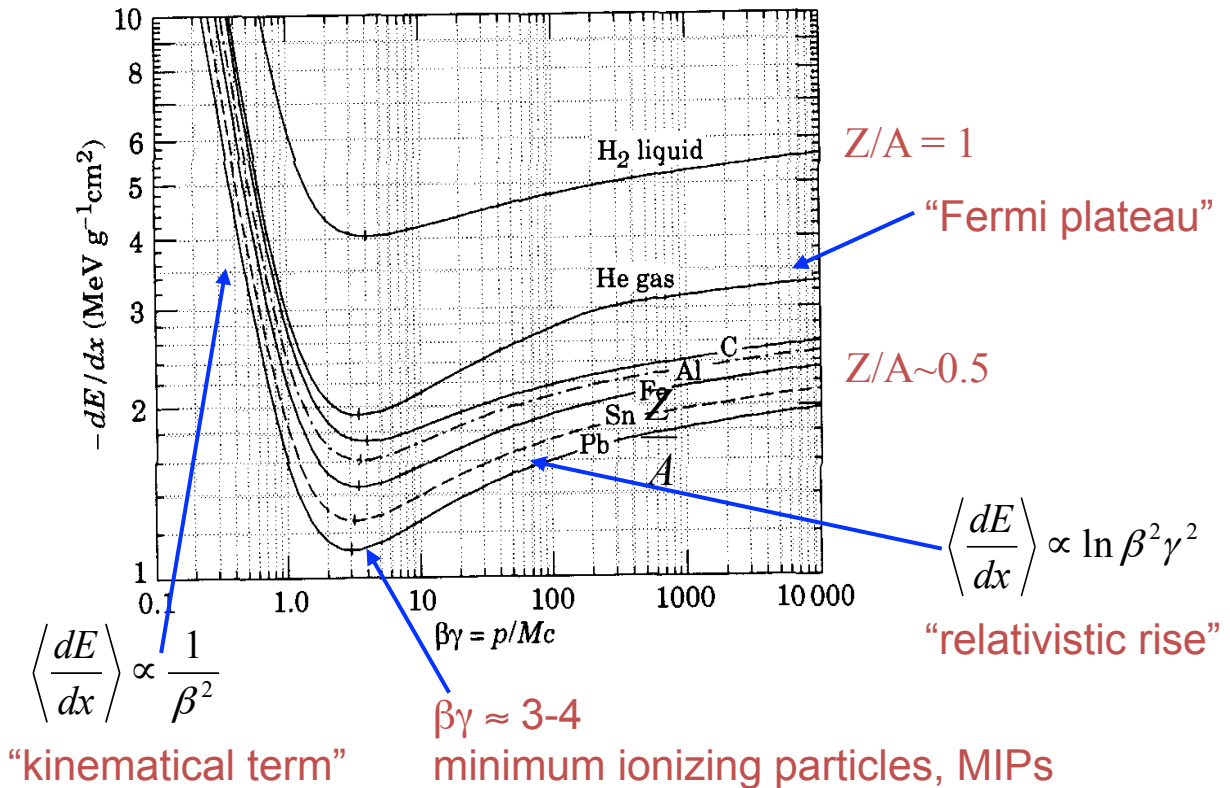
- How many encounters are there?
- Should be proportional to electron density in medium $N_e \propto \frac{Z}{A} N_A \cdot \rho$
- The real Bethe-Bloch formula

$$\left\langle \frac{dE}{dx} \right\rangle = -4\pi N_A r_e^2 m_e c^2 z^2 \frac{Z}{A} \frac{1}{\beta^2} \left[\frac{1}{2} \ln \frac{2m_e c^2 \gamma^2 \beta^2}{I^2} T^{\max} - \beta^2 - \frac{\delta}{2} \right]$$

- Energy loss by ionization only → **Bethe-Bloch formula**

$$\left\langle \frac{dE}{dx} \right\rangle = -4\pi N_A r_e^2 m_e c^2 z^2 \frac{Z}{A} \frac{1}{\beta^2} \left[\frac{1}{2} \ln \frac{2m_e c^2 \gamma^2 \beta^2}{I^2} T^{\max} - \beta^2 - \frac{\delta}{2} \right]$$

- dE/dx in [MeV g⁻¹ cm²]
- Strictly valid for “heavy” particles ($m \geq m_\mu$) only. For electrons, use Berger Seltzer formula
- dE/dx depends only on β , independent of m
- First approximation: medium simply characterized by $Z/A \sim$ electron density



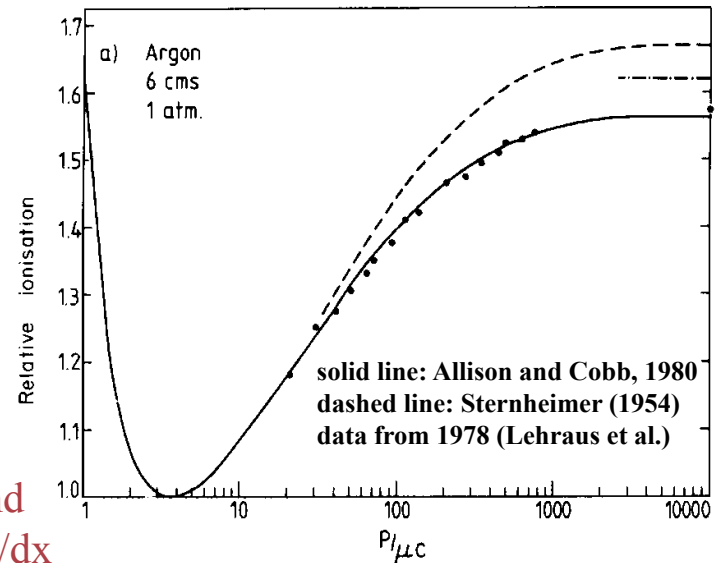
- Bethe-Bloch formula cont'd

$$\left\langle \frac{dE}{dx} \right\rangle = -4\pi N_A r_e^2 m_e c^2 z^2 \frac{Z}{A} \frac{1}{\beta^2} \left[\frac{1}{2} \ln \frac{2m_e c^2 \gamma^2 \beta^2}{I^2} T^{\max} - \beta^2 \frac{\delta}{2} \right]$$

- Relativistic rise - $\ln \gamma^2$ term - attributed to relativistic expansion of transverse E-field \rightarrow \rightarrow contributions from more distant collisions
- Relativistic rise cancelled at high γ by “density effect”, polarization of medium screens more distant atoms. Parameterized by δ (material dependent) \rightarrow Fermi plateau
- Formula takes into account energy transfers

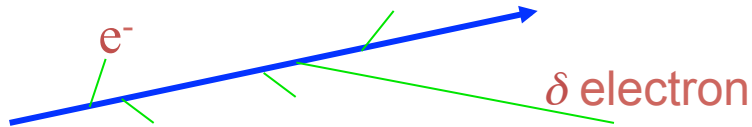
$$I \leq dE \leq T^{\max} \quad I \approx I_0 Z \quad \text{with } I_0 = 10 \text{ eV}$$

I : mean ionization potential, measured (fitted) for each element

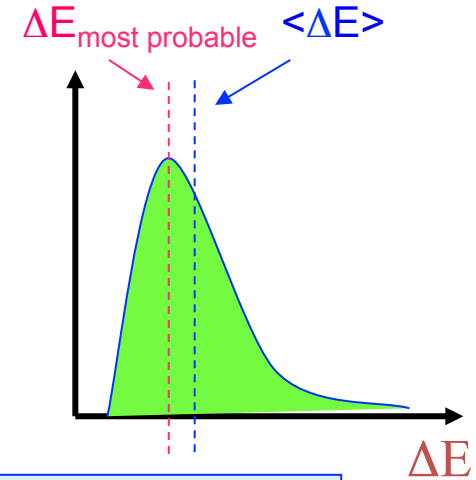


Measured and
calculated dE/dx

- Real detector (limited granularity) can not measure $\langle dE/dx \rangle$
It measures the energy ΔE deposited in a layer of finite thickness δx
- For thin layers or low density materials
Few collisions, some with high energy transfer

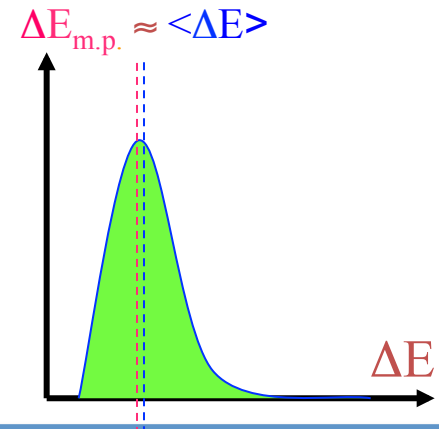
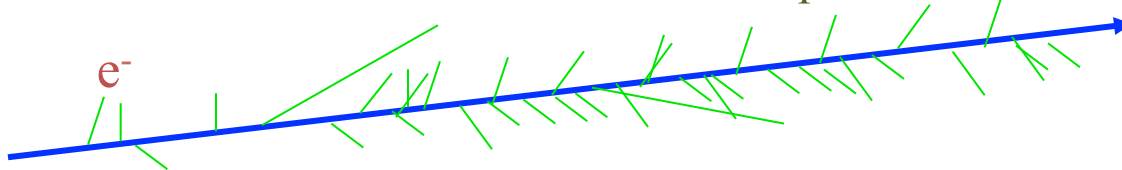


Energy loss distributions show large fluctuations towards high losses: **"Landau tails"**



Example: Si sensor 300 μm thick $\rightarrow \Delta E_{\text{most probable}} \sim 82 \text{ keV}$ $\langle \Delta E \rangle \sim 115 \text{ keV}$

- For thick layers and high density materials
Many collisions
Central Limit Theorem \rightarrow Gaussian shaped distributions



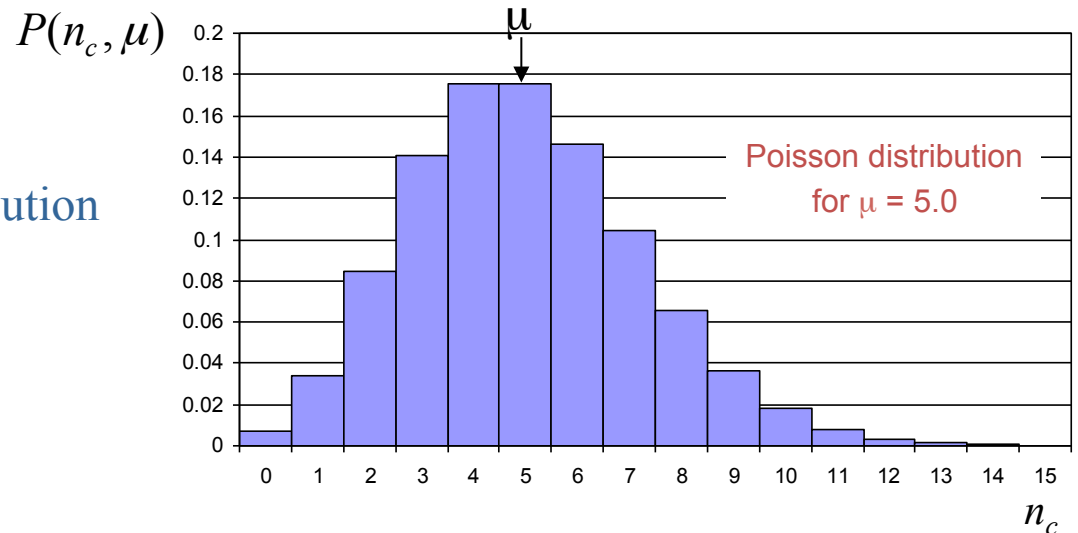
- Energy deposition in detectors happens in small discrete and independent steps.
- Even in the case of a well defined and constant amount of energy deposited in a detector, the achievable resolution in terms of energy, spatial coordinates or time is constrained by the statistical fluctuations in the number of charge carriers (**electron-hole pairs**, electron-ion pairs, scintillation photons) produced in the detector.
- In most cases, the number of charge carriers n_c is well described by a **Poisson distribution** with mean $\mu = \langle n_c \rangle$

$$P(n_c, \mu) = \frac{\mu^{n_c} e^{-\mu}}{n_c!}$$

- The variance of the Poisson distribution is equal to its mean value.

$$\sigma_{n_c}^2 = \langle n_c^2 \rangle - \langle n_c \rangle = \langle n_c \rangle = \mu$$

$$\sigma_{n_c} = \sqrt{\mu} \quad \text{standard deviation}$$



- For large μ values (> 10), as it is the case for silicon detectors, the Poisson distribution becomes reasonably well approximated by the symmetric and continuous **Gauss distribution**

$$G(n_c, \mu) = \frac{1}{\sqrt{2\pi}\sigma} \exp\left(-\frac{(n_c - \mu)^2}{2\sigma^2}\right)$$

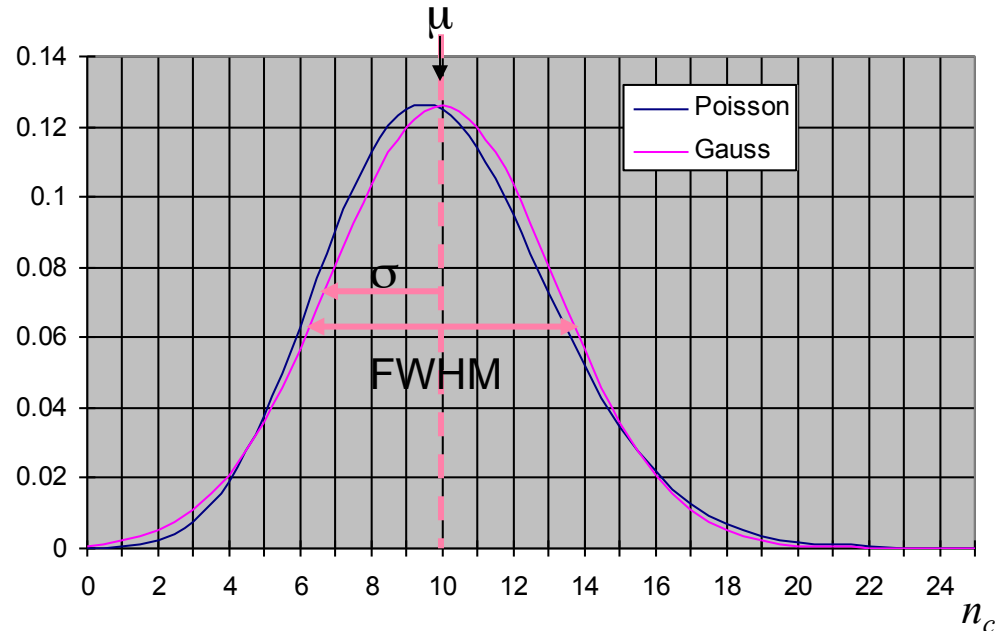
with $\sigma = \sqrt{\mu}$

FWHM is often used to characterize the detector resolution

$$\exp\left(-\frac{(n_c - \mu)^2}{2\sigma^2}\right) \equiv \frac{1}{2}$$

$$\rightarrow n_c - \mu = \sqrt{-2 \ln 0.5} \cdot \sigma$$

$$\text{FWHM} = 2(n_c - \mu) = 2.35 \cdot \sigma$$

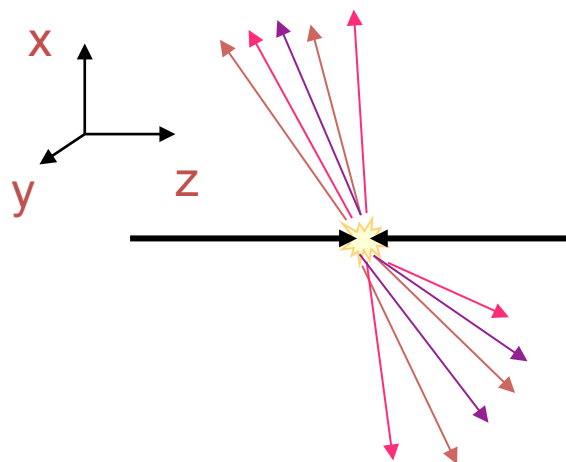


The energy resolution of many detectors is found to scale like

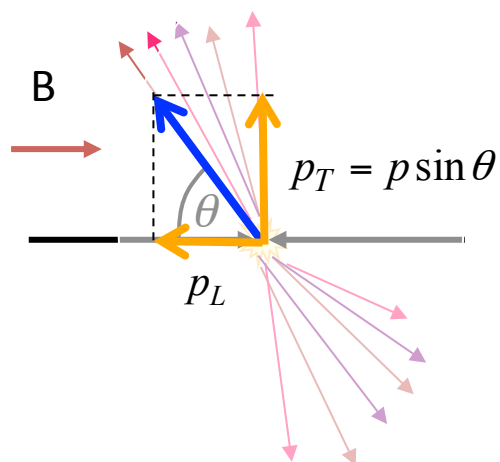
$$\sigma_E \propto \sqrt{\langle n_c \rangle} = \sqrt{\mu} \quad \rightarrow \quad \frac{\sigma_E}{E} \propto \frac{\sqrt{\mu}}{\mu} = \frac{1}{\sqrt{\mu}}$$

Often, also time and spatial resolution improve with increasing $\langle n_c \rangle$

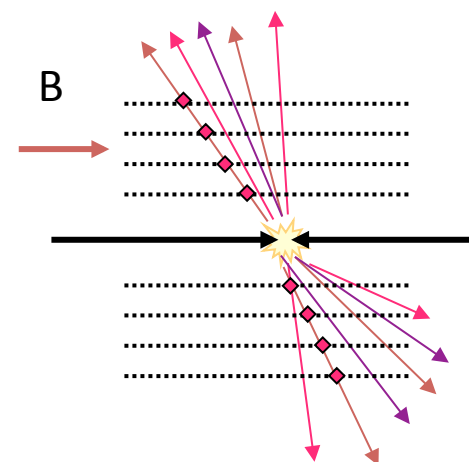
$$\frac{\sigma_{x,t}}{x,t} \propto \frac{1}{\sqrt{\mu}}$$



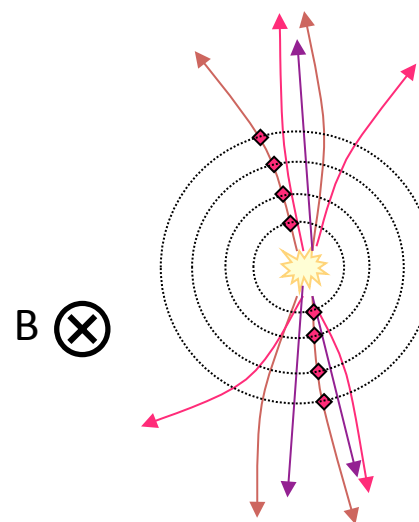
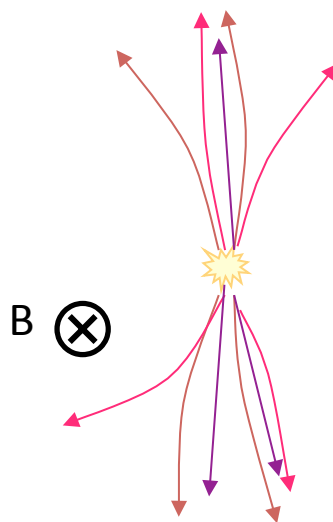
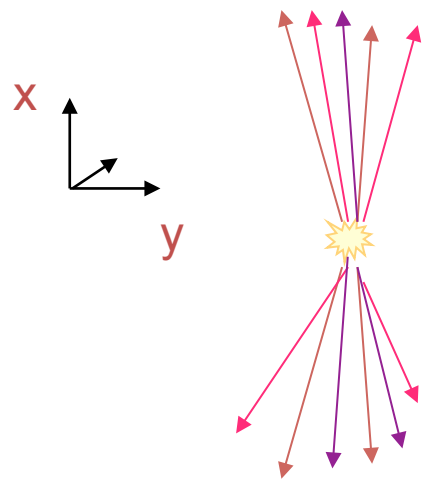
$B=0$

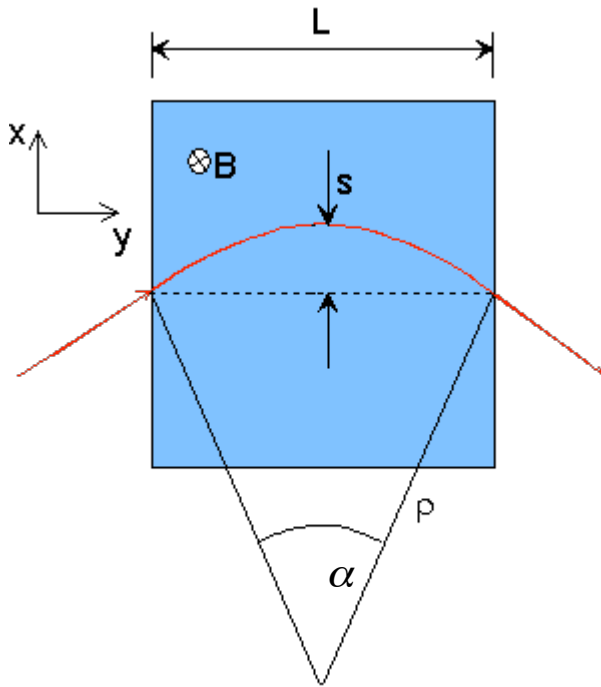


$B>0$



$B>0$





- We measure only p-component transverse to B field
 $L = \text{length of the detector (chord)}, s = \text{sagitta}, \rho = \text{bending radius}$

$$p_T = qB\rho \quad \rightarrow \quad p_T \text{ (GeV/c)} = 0.3B\rho \quad (\text{T} \cdot \text{m})$$

$$\frac{L}{2\rho} = \sin \alpha/2 \approx \alpha/2 \quad \rightarrow \quad \alpha \approx \frac{0.3L \cdot B}{p_T}$$

$$s = \rho(1 - \cos \alpha/2) \approx \rho \frac{\alpha^2}{8} \approx \frac{0.3}{8} \frac{L^2 B}{p_T}$$

the sagitta s is determined by 3 measurements with error $\sigma(x)$:

$$s = x_2 - \frac{x_1 + x_3}{2} \quad \left. \frac{\sigma(p_T)}{p_T} \right|^{meas.} = \frac{\sigma(s)}{s} = \frac{\sqrt{\frac{3}{2}}\sigma(x)}{s} = \frac{\sqrt{\frac{3}{2}}\sigma(x) \cdot 8p_T}{0.3 \cdot BL^2} \quad \boxed{\left. \frac{\sigma(p_T)}{p_T} \right|^{meas.} \propto \frac{\sigma(x) \cdot p_T}{BL^2}}$$

for N equidistant measurements, one obtains (R.L. Gluckstern, NIM 24 (1963) 381)

$$\left. \frac{\sigma(p_T)}{p_T} \right|^{meas.} = \frac{\sigma(x) \cdot p_T}{0.3 \cdot BL^2} \sqrt{720/(N+4)} \quad (\text{for } N \geq \sim 10)$$

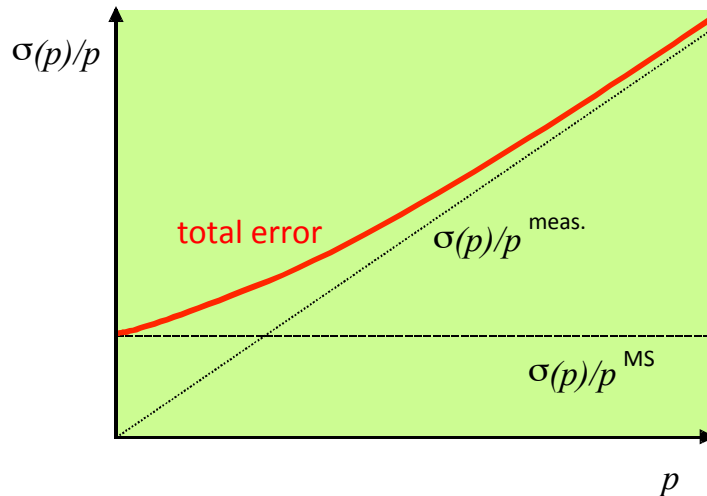
- What is the contribution of **multiple scattering** to $\frac{\sigma(p)}{p_T}$?

remember $\frac{\sigma(p)}{p_T} \propto \sigma(x) \cdot p_T$

$\sigma(x)|^{MS} \propto \theta_0 \propto \frac{1}{p}$

$\left. \begin{array}{l} \frac{\sigma(p)}{p_T} \propto \sigma(x) \cdot p_T \\ \sigma(x)|^{MS} \propto \theta_0 \propto \frac{1}{p} \end{array} \right\} \frac{\sigma(p)}{p_T} \Big|^{MS} = \text{constant} \quad \text{i.e. independent of } p$

More precisely: $\frac{\sigma(p)}{p_T} \Big|^{MS} = 0.045 \frac{1}{B\sqrt{LX_0}}$



Example:

$p_t = 1 \text{ GeV}/c, L = 1\text{m}, B = 1 \text{ T}, N = 10$

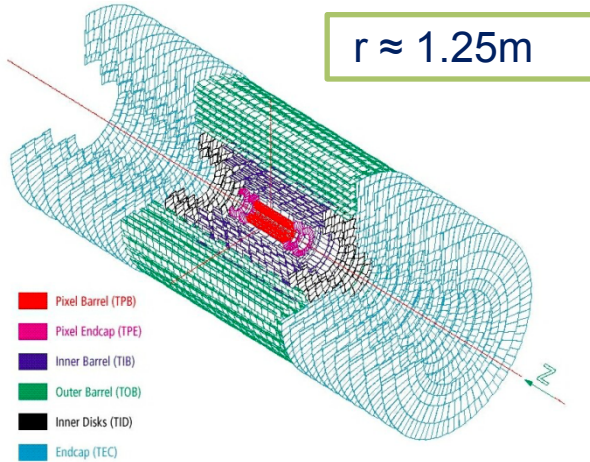
$\sigma(x) = 200 \mu\text{m} \quad \frac{\sigma(p_T)}{p_T} \Big|^{meas.} \approx 0.5\%$

Assume detector ($L = 1\text{m}$) to be filled with 1 atm. Argon gas ($X_0 = 110\text{m}$),

$\frac{\sigma(p)}{p_T} \Big|^{MS} \approx 0.5\%$

Optimistic, since a gas detector consists of more than just gas!

CMS Silicon Tracker



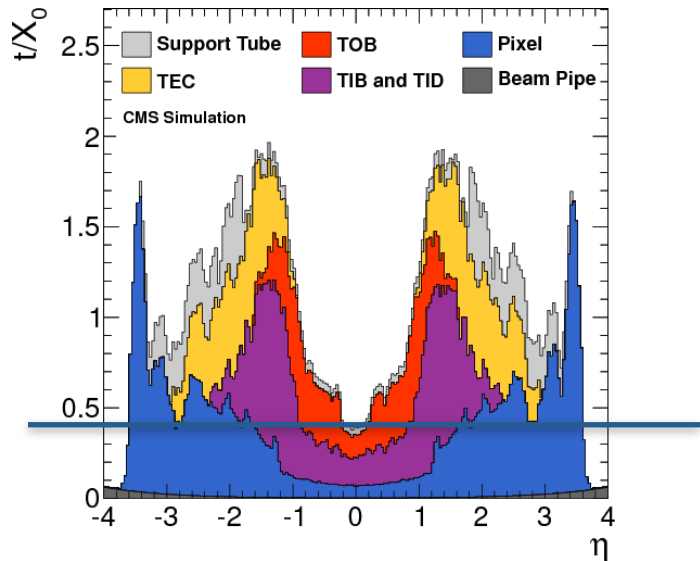
- $B = 3.8\text{T}$, $L = 1.25\text{m}$, average $N \approx 10$ layers
- Average resolution per layer $\approx 25\mu\text{m}$

$$\left. \frac{\sigma(p_T)}{p_T} \right|^{meas.} = \frac{\sigma(x) \cdot p_T}{0.3 \cdot BL^2} \sqrt{720/(N+4)}$$

$\sigma_p/p = 0.1\%$ momentum resolution (at 1 GeV)

$\sigma_p/p = 10\%$ momentum resolution (at 1 TeV)

Material budget (Si, cables, cooling pipes, support structure...)



- $B = 3.8\text{T}$, $L = 1.25\text{m}$, $t/X_0 \approx 0.4-0.5$ @ $\eta < 1$

$$\left. \frac{\sigma(p)}{p_T} \right|^{MS} = 0.045 \frac{1}{B\sqrt{LX_0}} = 0.045 \frac{1}{B \cdot L} \sqrt{\frac{t}{X_0}}$$

$\sigma_p/p = 0.7\%$ from multiple scattering

$$\text{pseudorapidity } \eta = -\ln\left(\tan\frac{\theta}{2}\right)$$

Silicon detectors are nowadays some of the most important
detectors in particle physics

They are widely used for tracking systems and for light sensing
in calorimetry

An introduction to their main properties and features

- Semiconductors widely used for charged particle and photon detection
- Sensor material – mainly silicon, III÷V materials also used

physical properties

availability

ease of use

cost

- Silicon technology is very mature

high quality crystal material

relatively low cost

although physical properties are not optimal for some specific applications

	I	II	III	IV	V	VI	VII	VIII
1	1 H							2 He
2	3 Li	4 Be	5 B	6 C	7 N	8 O	9 F	10 Ne
3	11 Na	12 Mg	13 Al	14 Si	15 P	16 S	17 Cl	18 Ar
4	19 K	20 Ca	31 Ga	32 Ge	33 As	34 Se	35 Br	36 Kr
5	37 Rb	38 Sr	49 In	50 Sn	51 Sb	52 Te	53 I	54 Xe
6	55 Cs	56 Ba	81 Tl	82 Pb	83 Bi	84 Po	85 At	86 Rn
7	87 Fr	88 Ra	113 Uut	114 Uuq	114 Uup	115 Uuh	117 Uus	118 Uuo

- Germanium
 - used in nuclear physics
 - needs cooling due to the small band gap (0.66 eV)
 - usually done with liquid nitrogen at 77 °K
- Silicon
 - can be operated at room temperature
 - synergy with microelectronics industry
 - standard material for vertex and tracking detectors in high energy physics
- Diamond
 - large band gap
 - requires no depletion zone
 - very radiation hard
 - drawback is a low signal and high cost

	Diamond	SiC (4H)	GaAs	Si	Ge
Atomic number Z	6	14/6	31/33	14	32
Bandgap E_g [eV]	5.5	3.3	1.42	1.12	0.66
$E(e-h \text{ pair})$ [eV]	13	7.6-8.4	4.3	3.6	2.9
density [g/cm ³]	3.515	3.22	5.32	2.33	5.32
e-mobility μ_e [cm ² /Vs]	1800	800	8500	1450	3900
h-mobility μ_h [cm ² /Vs]	1200	115	400	450	1900

Moderate band gap	$E_g = 1.12 \text{ eV} \Rightarrow E(\text{e-h pair}) = 3.6 \text{ eV}$ $\approx 30 \text{ eV}$ for e-ion in gas detectors, $\approx 100 \text{ eV}$ for photon in scintillators High carrier yield Better energy resolution and high signal
High specific density	$2.33 \text{ g/cm}^3 \rightarrow$ High specific energy loss dE/dx (M.I.P.) $\approx 3.8 \text{ MeV/cm}$, $\approx 108 \text{ e-h}/\mu\text{m}$ (average) Thin detectors Reduced range of secondary particles Better spatial resolution
High carrier mobility	$\mu_e = 1450 \text{ cm}^2/\text{Vs}$, $\mu_h = 450 \text{ cm}^2/\text{Vs}$ fast charge collection ($< 10 \text{ ns}$)
Very pure	$< 1 \text{ ppm}$ impurities and $< 0.1 \text{ ppb}$ electrical active impurities
Rigidity	allows thin self supporting structures
Detector production	by microelectronic techniques well known industrial technology, relatively low price, small structures workable
High intrinsic radiation hardness	

NB: The following concepts apply to any IV group elemental semiconductor (i.e. C, Si, Ge)

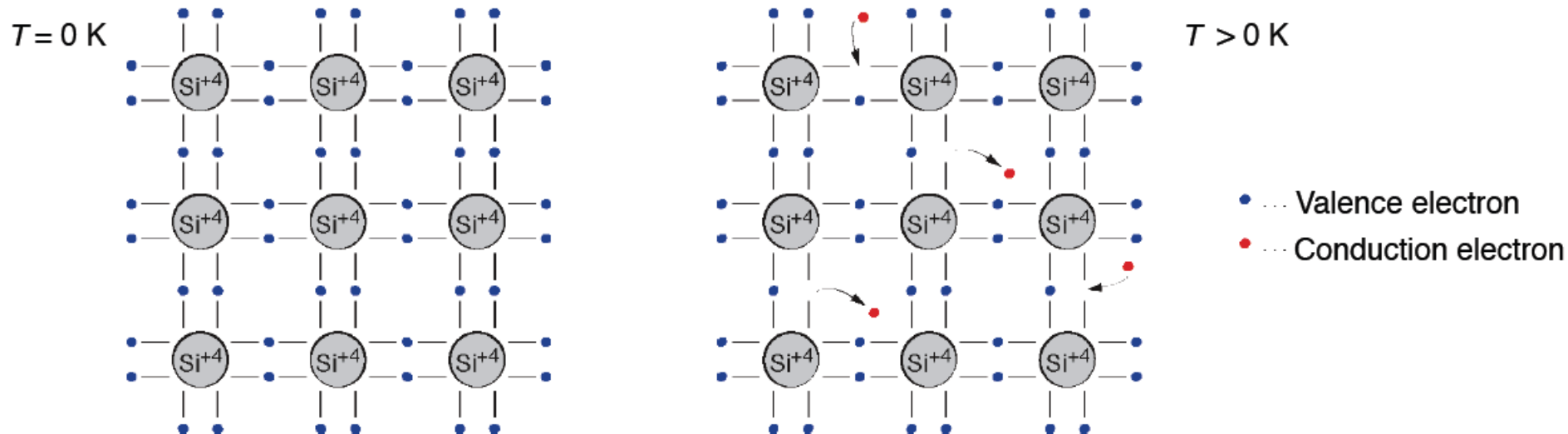
- Each atom has 4 closest neighbors, the 4 electrons in the outer shell are shared and form covalent bonds

Low temperature \rightarrow all electrons are bound

Higher temperature \rightarrow thermal vibrations break some of the bonds

free e^- cause conductivity (**electron conduction**)

remaining open bonds attract other $e^- \rightarrow$ “holes” change position (**hole conduction**)

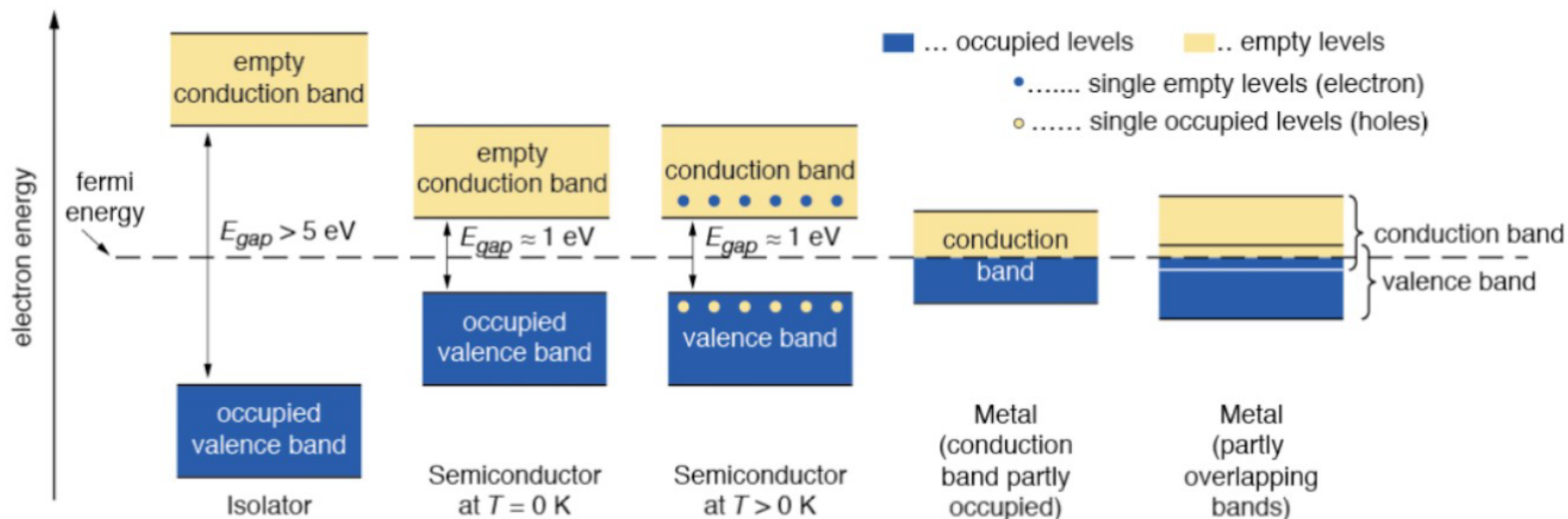


- In isolated atoms the electrons have only discrete energy levels
- Due to lattice symmetry, in solid state material the atomic levels merge to energy bands

Isolators → large energy gap (band gap) between conduction and valence bands

Semiconductors → small energy gap between conduction and valence bands

Metals → conduction and valence bands overlap



- Due to the small band gap, in semiconductors electrons can be excited already at room temperature and thus occupy the conduction band.
- Electrons from the conduction band may recombine with holes.
- A thermal equilibrium is reached between excitation and recombination:

charge carrier concentration: $n_e = n_h = n_i$ (charge neutrality)

- n_i is called intrinsic carrier concentration:

$$n_i = \sqrt{N_C N_V} \cdot \exp\left(-\frac{E_g}{2kT}\right) \propto T^{\frac{3}{2}} \cdot \exp\left(-\frac{E_g}{2kT}\right)$$

N_C and N_V are the number of admitted states in conduction and valence band, respectively (Fermi-Dirac statistics)

- In ultrapure silicon the intrinsic carrier concentration at $T \approx 300$ °K is $n_i = 1.45 \cdot 10^{10} \text{ cm}^{-3}$
taking into account approximately $10^{22} \text{ Atoms/cm}^3 \rightarrow 1$ in 10^{12} silicon atoms is ionized.

Drift velocity

electrons

$$\vec{v}_n = -\mu_n \cdot \vec{E}$$

holes

$$\vec{v}_p = \mu_p \cdot \vec{E}$$

e = electron charge

E = external electric field

m_n, m_p = effective mass of e^- and h^+

τ_n, τ_p = mean free time between collisions
for e^- and h^+ (carrier lifetime)

n_e, n_h = charge carrier density for e^- and h^+

Mobility

electrons

$$\mu_n = \frac{e \tau_n}{m_n}$$

holes

$$\mu_p = \frac{e \tau_p}{m_p}$$

$\approx 1450 \text{ cm}^2/\text{Vs}$

$\approx 450 \text{ cm}^2/\text{Vs}$

Si, 300 °K

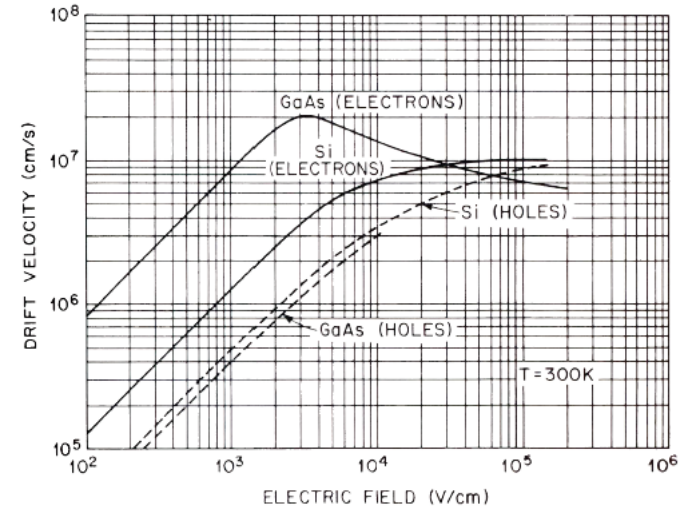
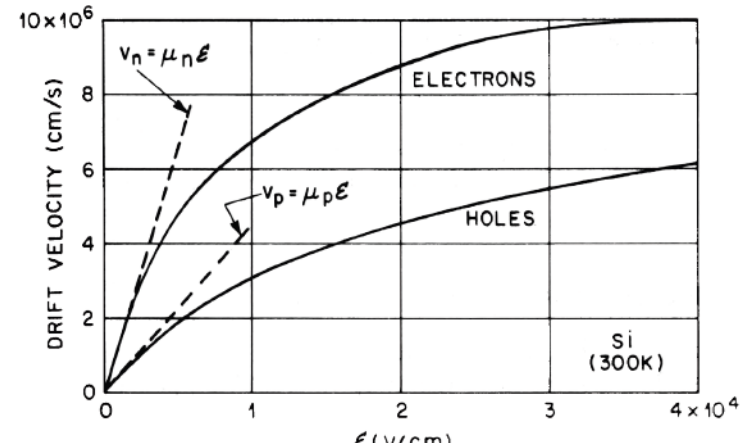
Resistivity

$$\rho = \frac{1}{e(\mu_n n_e + \mu_p n_h)}$$

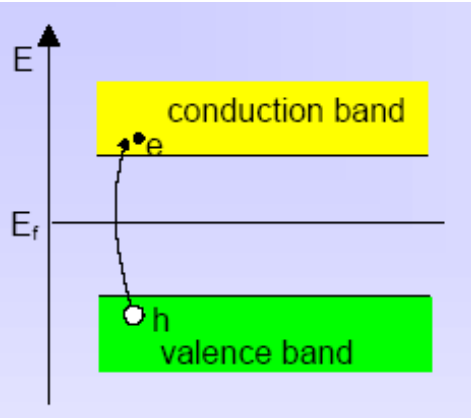
Intrinsic carrier concentration in pure silicon at $T \approx 300 \text{ °K}$

$$n_e = n_h = n_i = 1.45 \cdot 10^{10} \text{ cm}^{-3}$$

corresponding to an intrinsic resistivity of $\rho = 230 \text{ k}\Omega\text{cm}$



How to obtain a signal?



Pure (undoped) Silicon at $T = 300 \text{ °K}$

Intrinsic charge carrier density

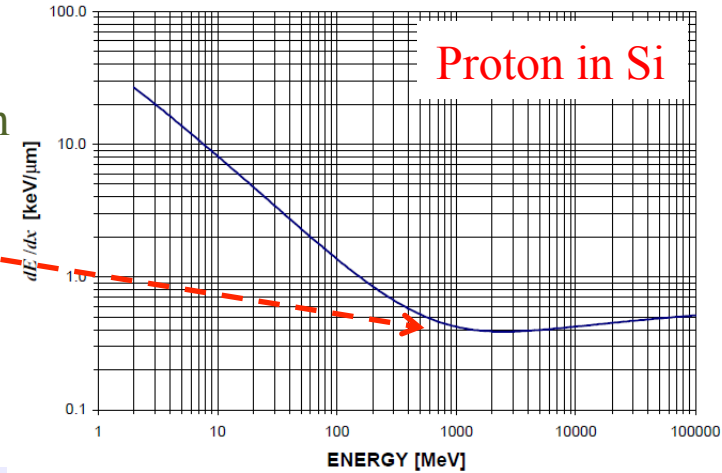
$$n_e = n_h = n_i \approx 1.45 \cdot 10^{10} \text{ cm}^{-3}$$

Mean ionization energy

$$I_0 = 3.62 \text{ eV,}$$

Mean energy loss per flight path of a mip

$$dE/dx = 3.87 \text{ MeV/cm}$$



Assuming a detector with a thickness of $d=300 \text{ μm}$ and an area of $A = 1 \text{ cm}^2$

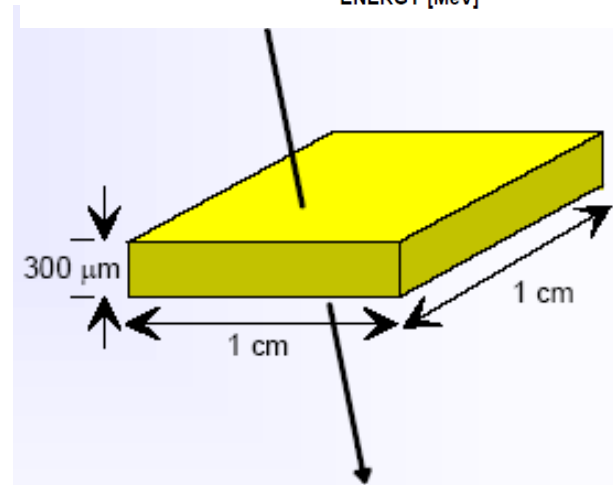
Charge signal of a mip

$$\frac{dE/dx \cdot d}{I_0} = \frac{3.87 \cdot 10^6 \text{ eV/cm} \cdot 0.03 \text{ cm}}{3.62 \text{ eV}} \approx 3.2 \cdot 10^4 \text{ e}^- \text{h}^+ \text{-pairs}$$

Intrinsic charge carriers

$$n_i \cdot d \cdot A = 1.45 \cdot 10^{10} \text{ cm}^{-3} \cdot 0.03 \text{ cm} \cdot 1 \text{ cm}^2 \approx 4.35 \cdot 10^8 \text{ e}^- \text{h}^+ \text{-pairs}$$

The number of thermal created $\text{e}^- \text{h}^+$ pairs is 4 order of magnitude larger than the signal!!!



Result:

The number of thermal created e^-h^+ pairs, i.e. the noise, is 4 order of magnitude larger than the signal

One of the most important parameter of a detector is the Signal to Noise Ratio (SNR)

A good detector should have a large SNR

This leads to two contradictory requirements:

Large Signal \rightarrow low ionization energy, i.e small band gap

Low Noise \rightarrow very few intrinsic charge carriers, i.e. large band gap

Solution

Reduce number of free charge carrier in the sensitive volume

How:

Depleted zone in reverse biased pn junction

Most silicon detectors make use of reverse biased p-n junctions

- Doping is the replacement of a small number of atoms in the lattice by atoms of neighboring columns from the periodic table

In case of Si (IV column), mostly used Pb, As, Sb from V column and B, Al, Ga, In from III column

- These doping atoms create energy levels within the band gap and therefore modify the conductivity

- Definitions

An un-doped semiconductor is called an **intrinsic semiconductor**

For each conduction electron exists the corresponding hole

A doped semiconductor is called an **extrinsic semiconductor**

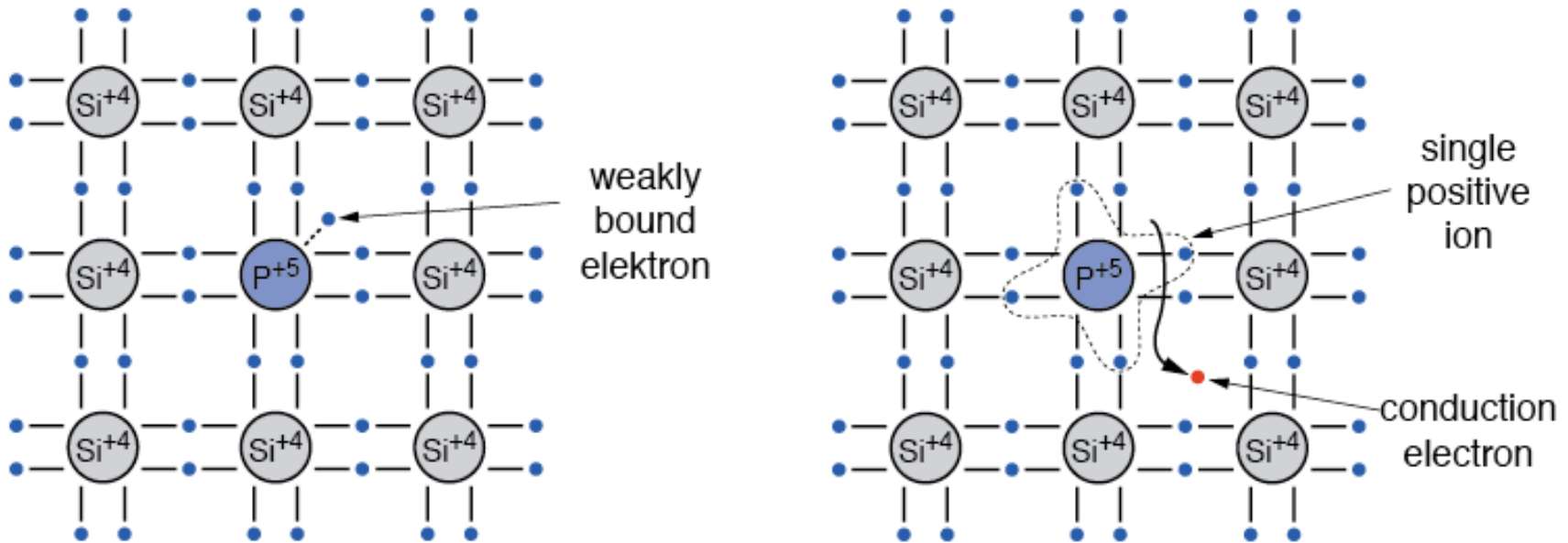
Extrinsic semiconductors have an abundance of electrons or holes

- n-type silicon

Add elements from V group (e.g. P, As, Sb)

The 5th valence electron is weakly bound and thus can be easily released

Doping atoms are called **donors**

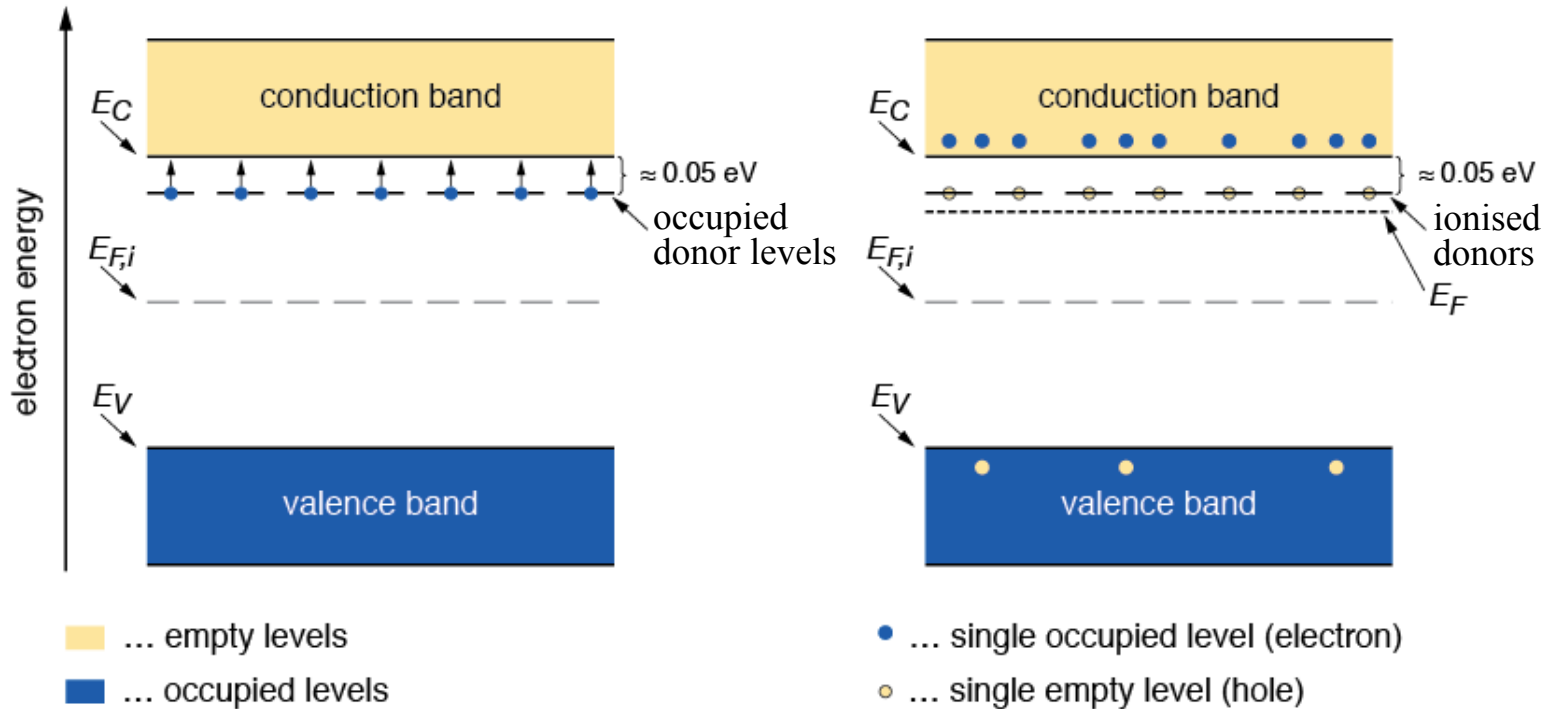


- Negatively charged **electrons** are the majority carriers

The released conduction electron leaves a positively charged ion →

→ **positive space charge**

- The energy level of the donor is just below the edge of the conduction band
At room temperature most electrons are raised to the conduction band
The Fermi level E_F moves up

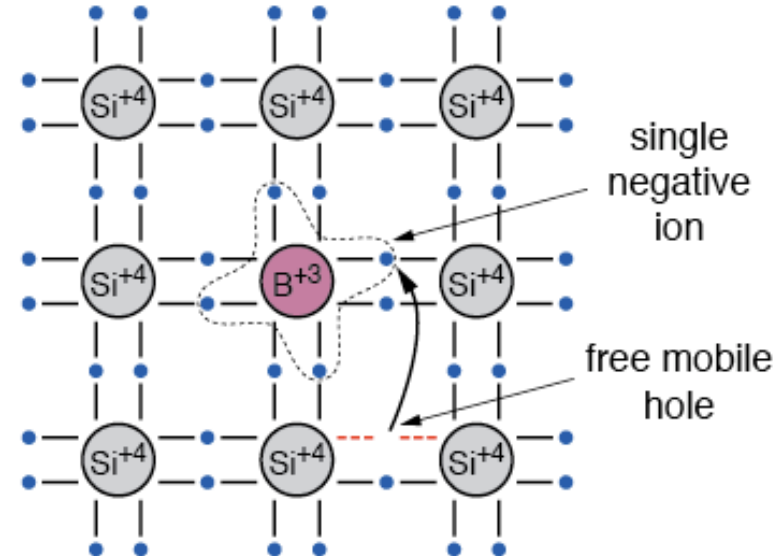
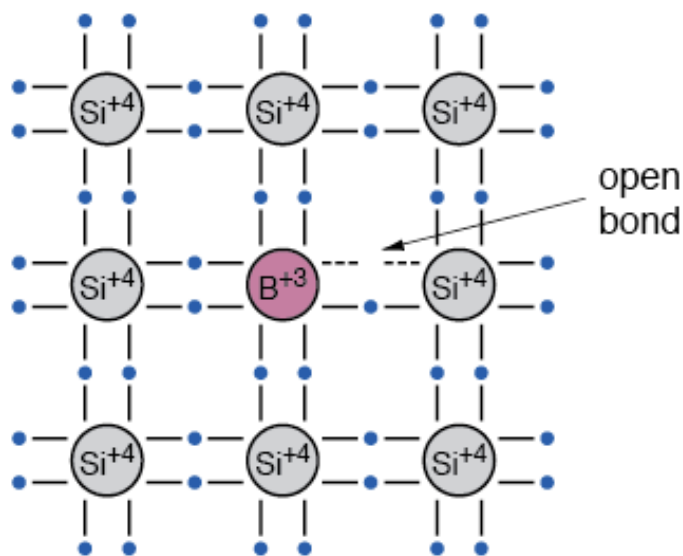


- p-type silicon

Add elements from III group (e.g. B, Al, Ga, In)

One valence bond remains open and thus attract electrons from neighbor atoms

Doping atoms are called **acceptors**



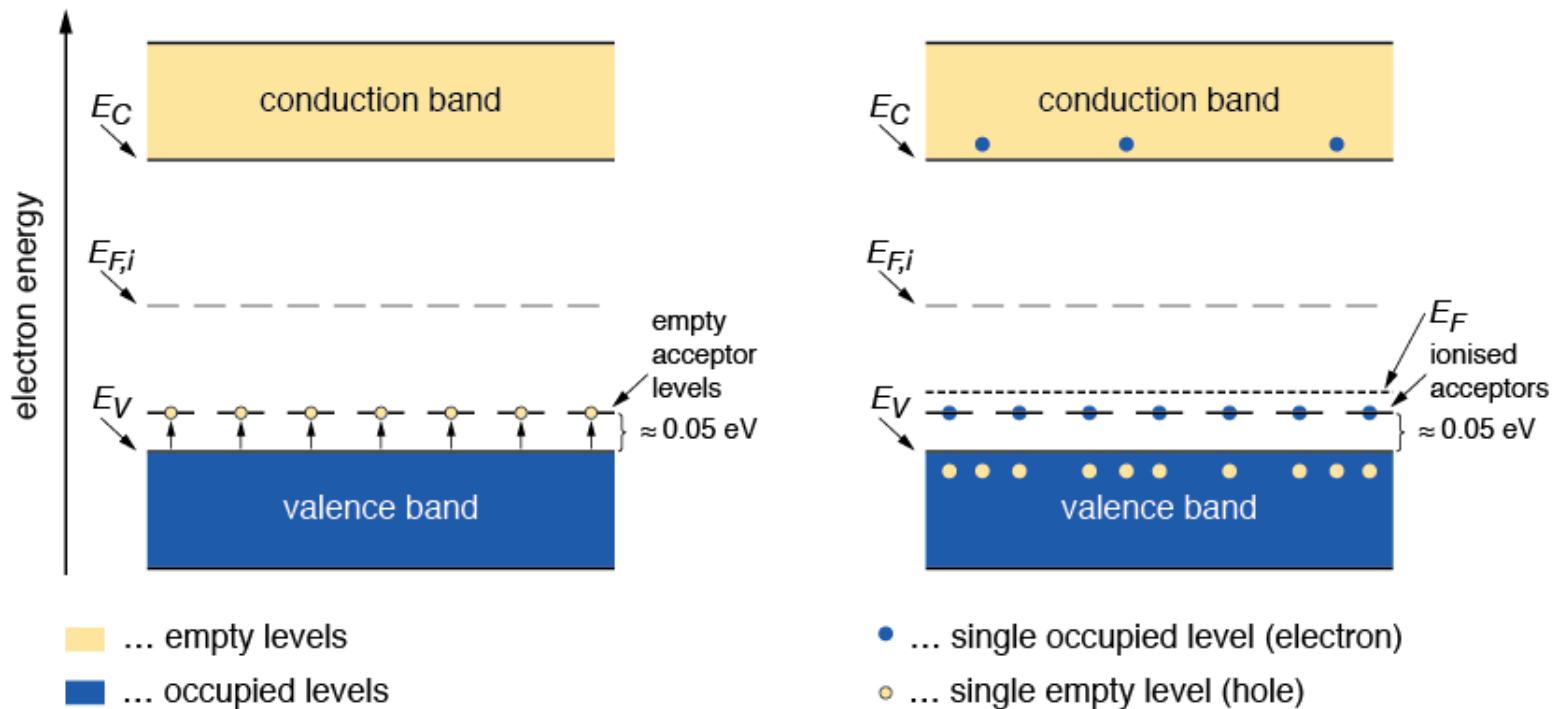
- Positively charged **holes** are the majority carriers

The acceptor atom in the lattice becomes a negatively charged ion →

→ **negative space charge**

- The energy level of the acceptor is just above the edge of the valence band
At room temperature most levels are occupied by electrons leaving holes in the valence band

The Fermi level E_F moves down



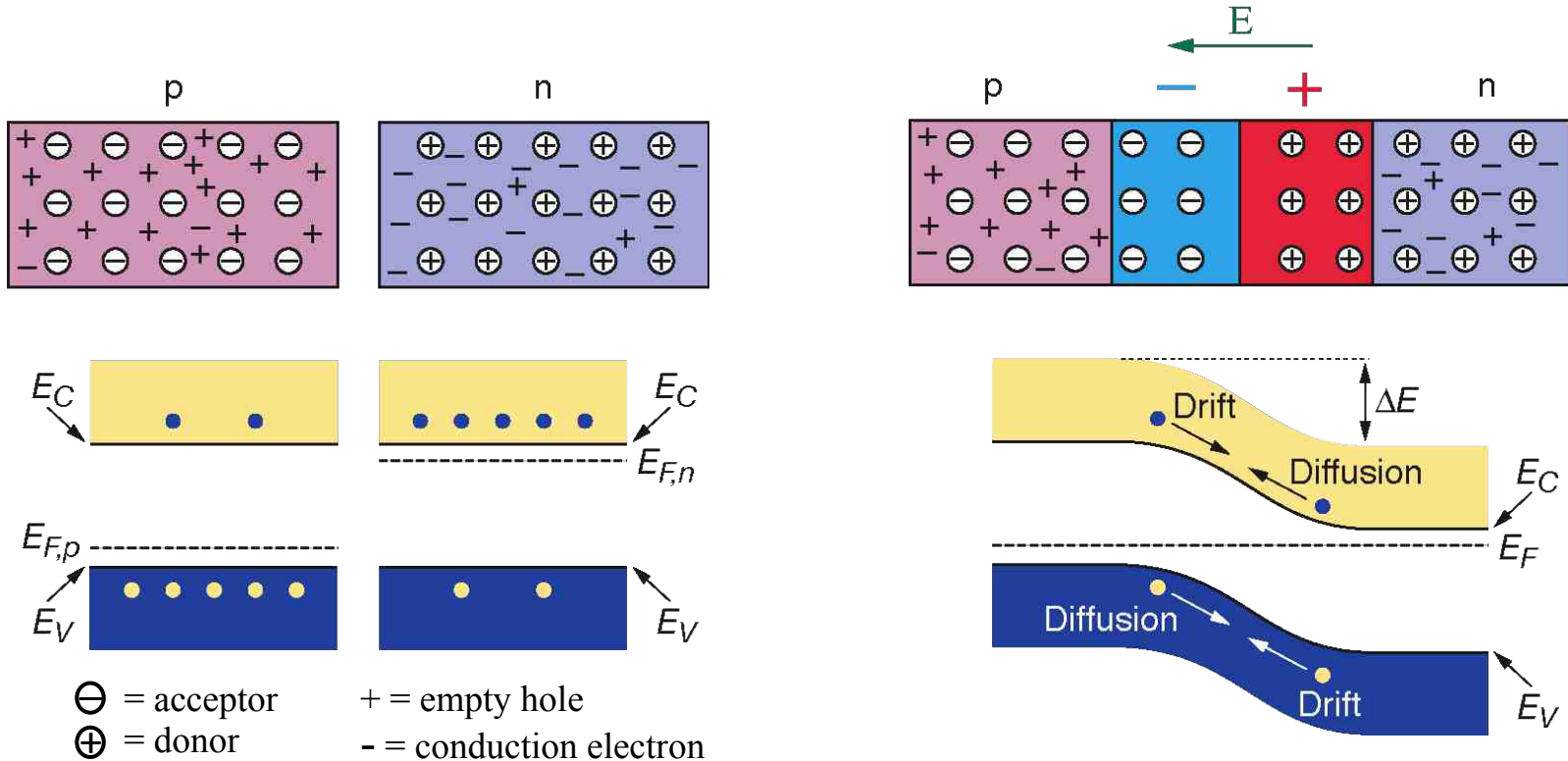
The p-n junction

- Interface of an n-type and p-type semiconductor

The difference in the Fermi levels cause diffusion of excessive carriers towards the other material until thermal equilibrium is reached and the Fermi level is equal

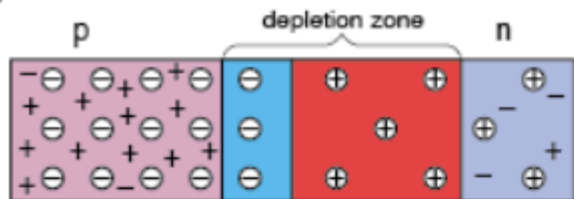
The remaining (fixed) ions create a space charge region and an electric field stopping further diffusion

- The stable space charge region is free of charge carriers and is called **depletion zone**



Electrical properties of a p-n junction

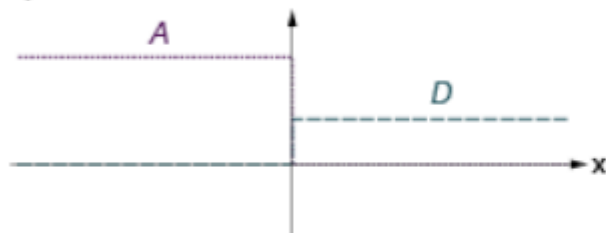
pn junction scheme



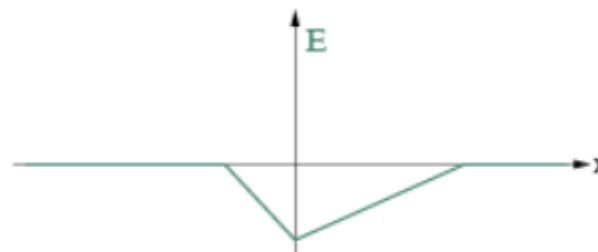
concentration of free charge carriers



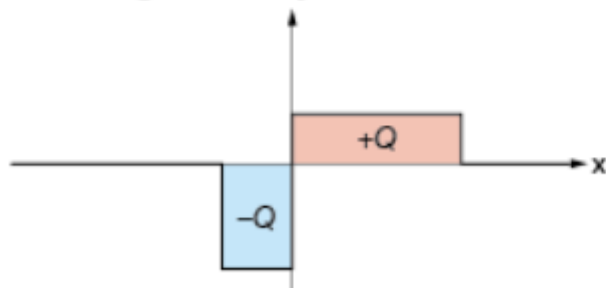
acceptor and donator concentration



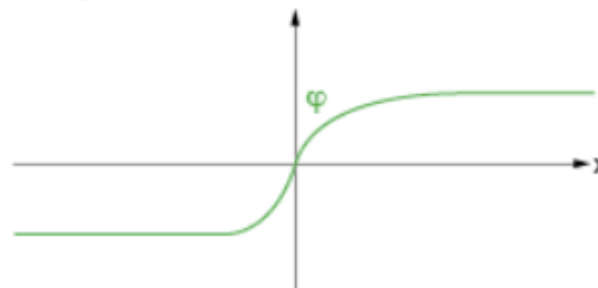
electric field



space charge density



electric potential

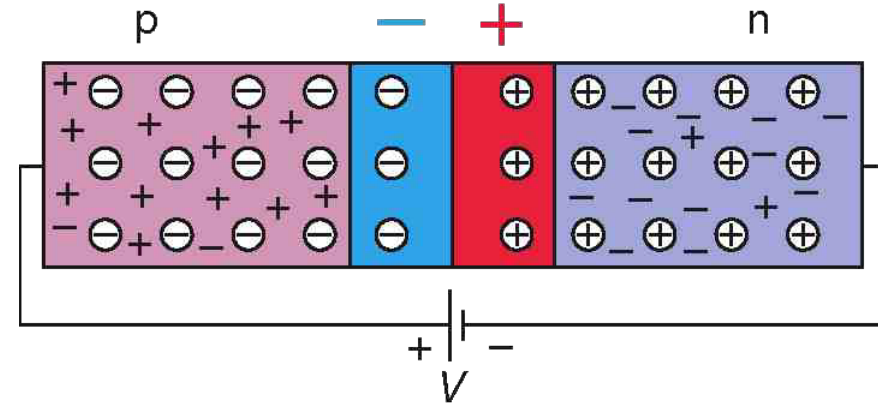


- ⊖ = acceptor
- ⊕ = donor
- + = empty hole
- = conduction electron

- Apply an external voltage V with the anode to p and the cathode to n

e^- and holes are refilled to the depletion zone

The depletion zone becomes **narrower**

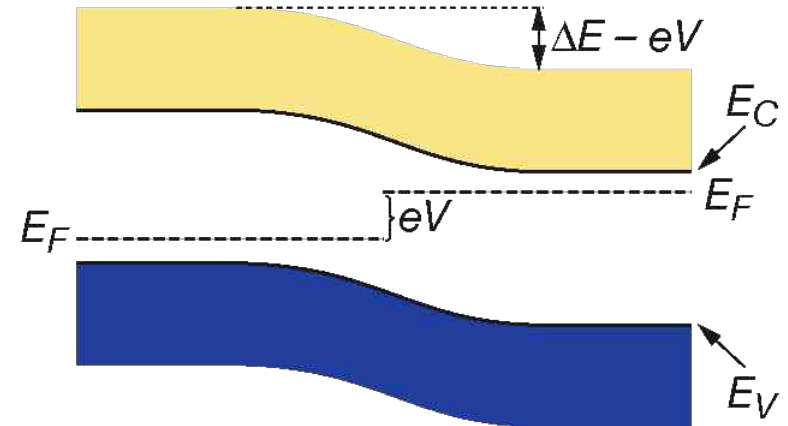


- Consequences:

The potential barrier becomes smaller by $\sim eV$

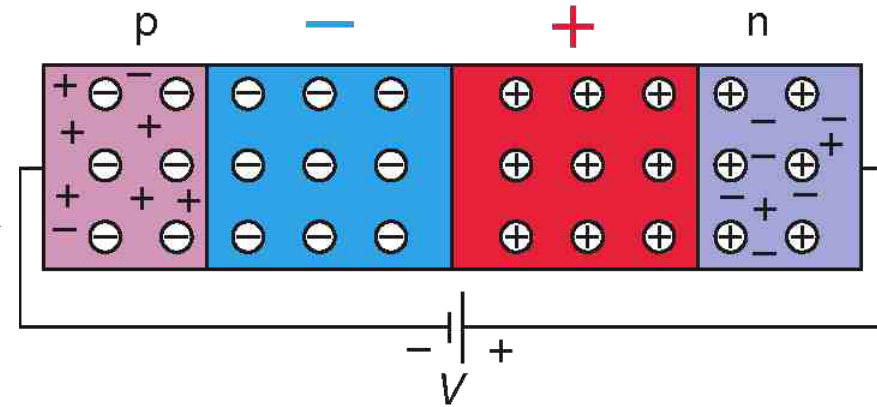
Diffusion across the junction becomes easier

The current across the junction increases significantly

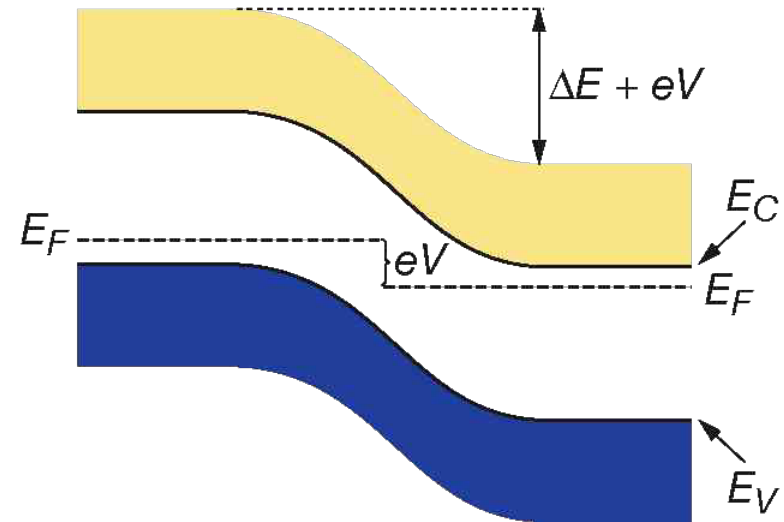


p-n junction with forward bias

- Apply an external voltage V with the cathode to p and the anode to n
 - e^- and holes are pulled out of the depletion zone
 - The depletion zone becomes **larger**



- Consequences:
 - The potential barrier becomes higher by $\sim eV$
 - Diffusion across the junction is suppressed
 - The current across the junction is very small (“leakage current”)



This is the way we usually operate our semiconductor detectors!

p-n junction with reverse bias

Example of a typical p⁺-n junction in a silicon detector

- Effective doping concentration in typical silicon detector with p⁺-n junction

$$N_a = 10^{15} \text{ cm}^{-3} \text{ in p}^+ \text{ region}$$

$$N_d = 10^{12} \text{ cm}^{-3} \text{ in n bulk}$$

- Width without external voltage

$$W_p = 0.02 \text{ } \mu\text{m}$$

$$W_n = 23 \text{ } \mu\text{m}$$

- Applying a reverse bias voltage of 100 V

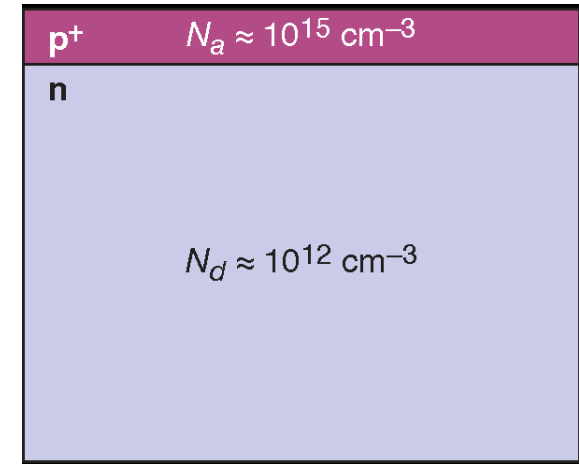
$$W_p = 0.4 \text{ } \mu\text{m}$$

$$W_n = 363 \text{ } \mu\text{m}$$

- Width of depletion zone in n bulk

$$W = \sqrt{2\varepsilon_0\varepsilon_r\mu\rho|V|} \quad \text{with} \quad \rho = \frac{1}{e\mu N_{\text{eff}}}$$

Derived by solving Poisson equation with $N_a \gg N_d$



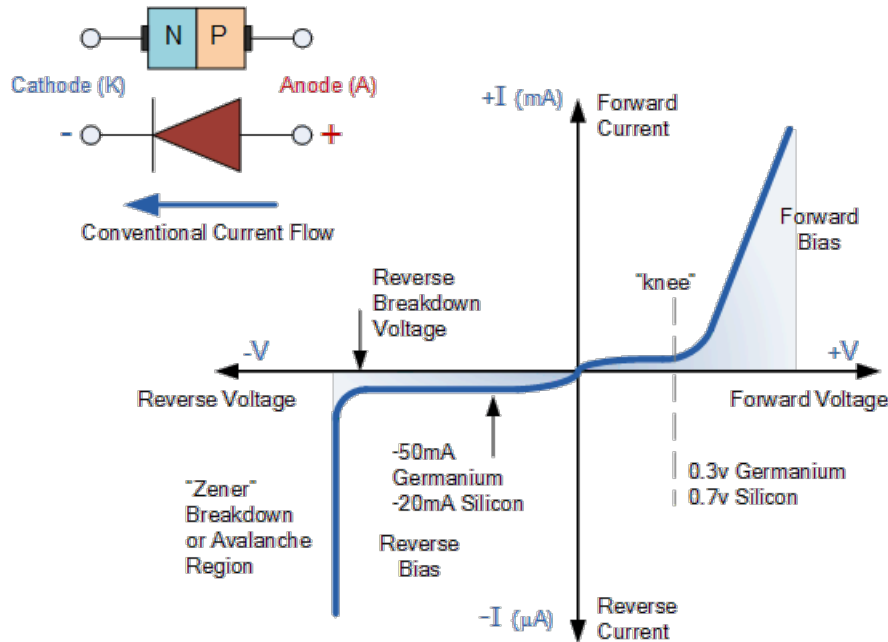
p⁺-n junction

V = External voltage!
 ρ = specific resistivity
 μ = mobility of majority charge carriers
 N_{eff} = effective doping concentration

- Typical current-voltage of a p-n junction (diode)

Exponential current increase in forward bias

Small saturation in reverse bias



Ideal diode equation

$$I = I_0 \left(e^{\frac{qV}{kT}} - 1 \right)$$

I = the net current flowing through the diode
 I_0 = dark or reverse saturation current, the diode leakage current density in the absence of light
 V = applied voltage across the terminals of the diode
 q = absolute value of electron charge
 k = Boltzmann's constant
 T = absolute temperature (K).

- The "dark saturation current" I_0 is an extremely important parameter which differentiates one diode from another
- I_0 is a measure of the recombination in a device

A diode with a larger recombination will have a larger I_0

Leakage current of a p-n junction

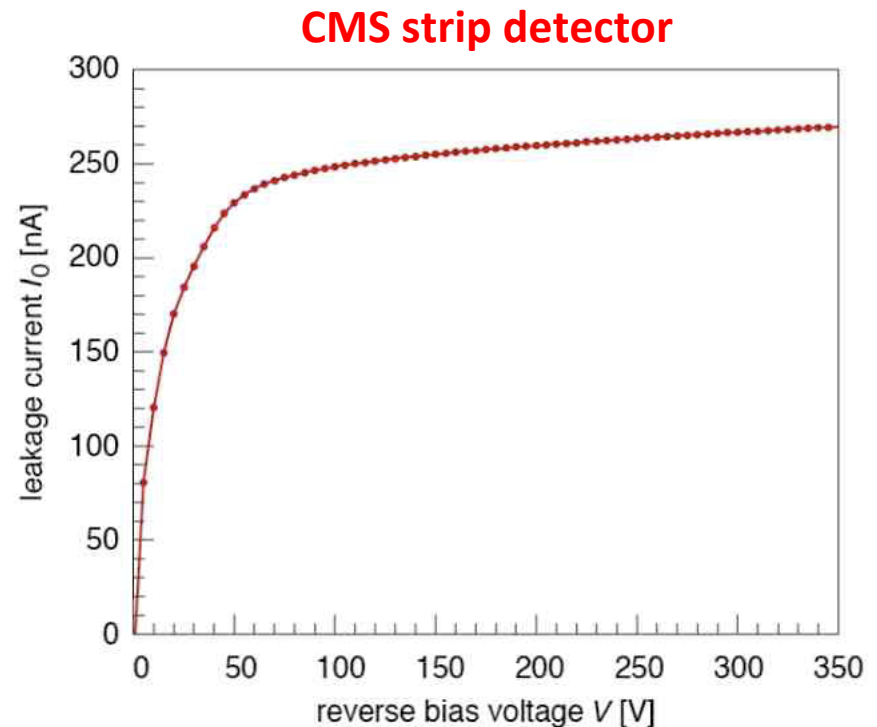
- A silicon detector is operated with reverse bias, hence the reverse saturation current I_0 (leakage current) is a relevant figure of merit

I_0 is dominated by thermally generated e^-h^+ pair

Due to the applied electric field e^-h^+ pair cannot recombine and are separated

The drift of the e^- and h^+ to the electrodes causes the leakage current

*Leakage current of CMS strip detector
measured at room temperature*



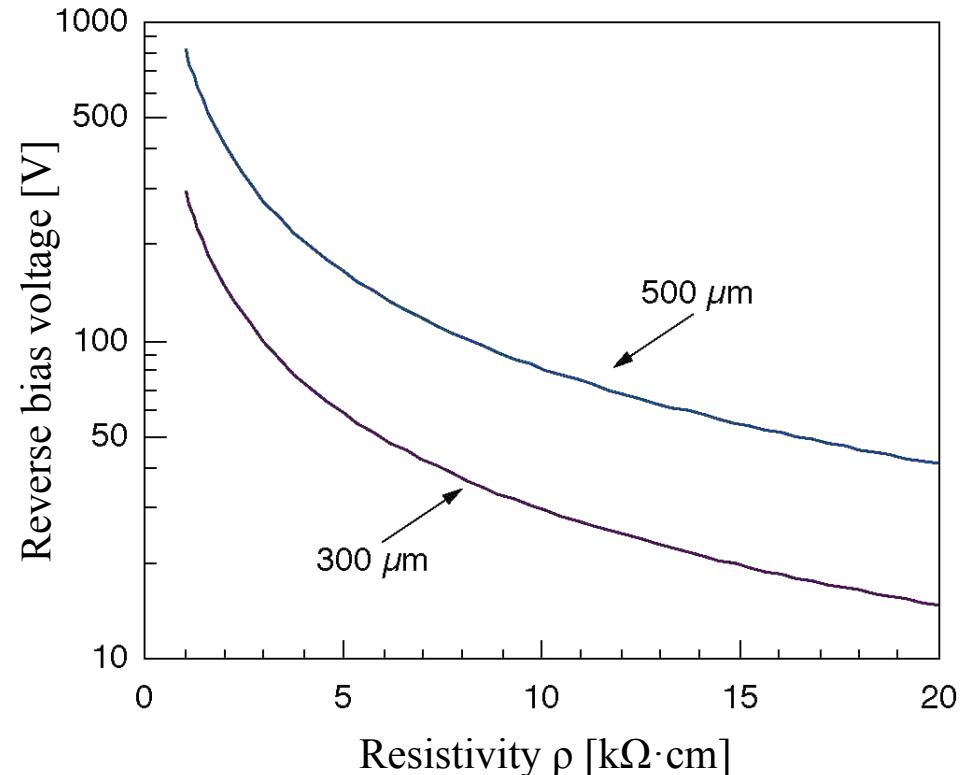
Depletion voltage of a p-n junction

- The depletion voltage is the minimum voltage at which the bulk of the sensor is fully depleted

The operating voltage is usually chosen to be slightly higher (overdepletion)

High resistivity material (i.e. low doping) requires low depletion voltage

Depletion voltage as a function of the material resistivity for two different detector thicknesses (300 μm , 500 μm)



- The detector capacitance for a typical Si p-n junction ($N_a \gg N_d \gg n_i$) the detector capacitance is given as

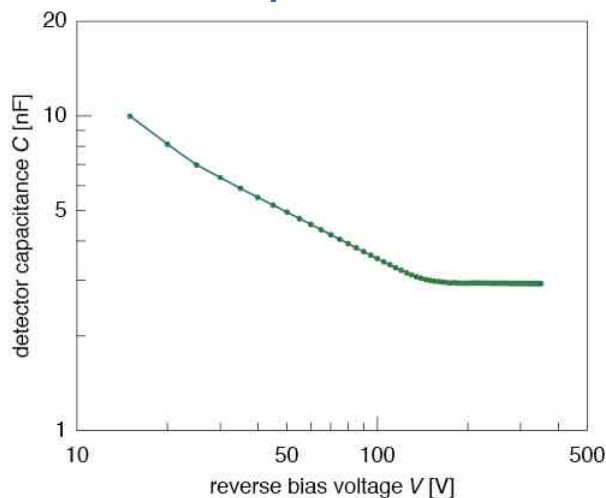
$$C = \sqrt{\frac{\epsilon_0 \epsilon_r}{2 \mu \rho |V|}} \cdot A$$

ρ = specific resistivity of the bulk
 μ = mobility of majority charge carrier
 V = bias voltage
 A = detector surface

Capacitance is similar to parallel-plate capacitor

Fully depleted detector capacitance defined by geometric capacitance

Measured detector capacitance as a function of the bias voltage of CMS strip detector



The depletion voltage can be determined by measuring the capacitance versus the reverse bias voltage.

